HYDRODYNAMICS STUDIES IN TWO- AND THREE- PHASE BUBBLE COLUMNS

MAY KHIN THET

NATIONAL UNIVERSITY OF SINGAPORE

2004

HYDRODYNAMICS STUDIES IN TWO- AND THREE- PHASE BUBBLE COLUMNS

MAY KHIN THET

(B.E., Yangon Technological University)

A THESIS SUBMITTED

FOR THE DEGREE OF MASTER OF ENGINEERING

DEPARTMENT OF CHEMICAL & BIOMOLECULAR ENGINEERING

NATIONAL UNIVERSITY OF SINGAPORE

2004

ACKNOWLEDGEMENT

I wish to record with genuine appreciation my indebtedness to my supervisor, Associate Professor Wang Chi-Hwa for his valuable advice and excellent guidance in the course of this investigation, preparation of this manuscript and above all his understanding and help in different ways, all the time.

Particularly, my deepest appreciation is expressed to my co-supervisor Associate Professor Reginald Beng Hee Tan for his constructive advice, helpful comments on the manuscript and help in the preparation of experiments right through the course of this work. Without him, this project could not have been completed.

I would also like to express my sincere thanks to all the technical and clerical staffs in the Chemical & Biomolecular Engineering Department, especially Ms. Sylvia, Mr. Boey Kok Hong, Ms. Lee Chai Keng, Ms. Samantha Fam, for their patient and help in purchasing chemicals, collecting glassware and setting up of experimental apparatus as well as guidance in using analytical instruments through the course of this work.

I really appreciate all the technical and clerical staff in the Chemical & Biomolecular Engineering Department for their patient especially to Mr. Ng Kim Poi and his staff for their help in setting up the experimental apparatus.

I am grateful to my colleagues, especially to Research fellow Dr. Deng Rengsheng and Dr. Yao Jun who always had an open ear for my troubles and by asking the right questions helped me understand some of the more complicated project aspect better myself.

Finally, I could not leave to say special thanks to my parents U Khin Maung Lwin and Daw Khin Kyaw, my brother and sisters, and my beloved friend Mr. San Linn Nyunt for their love and encouragement through out my master program. I wouldn't be a graduate without their support.

Last but not least, I would especially like to thank the National University of Singapore, for the award of a research scholarship and the Department of Chemical and Biomolecular Engineering for providing the necessary facilities for my MEng program.

TABLE OF CONTENTS

SUMMARY

Hydrodynamics behavior in bubble column is analyzed with various influencing factors such as solid particle type, concentration, liquid viscosity and liquid height. The onset of transition is examined by the static pressure difference and is characterized by the Wallis (1969) drift-flux model. Transition regime is found to be earlier with increasing viscosity, by the addition of large particles or under the condition of higher aspect ratio.

Liquid flow structure in the fully aerated bubble column is investigated using PIV (Particle Image Velocimetry) technique. The development of vortical structure near the wall can be eliminated by the presence of draught tube inside the bubble column. That leads the uniform normal stresses across the column and a pure descending region at wall region.

Liquid flow structure in the partially aerated bubble column is examined by varying the number and placement of aeration modes. Number of vortices reduces with asymmetrical aeration, and symmetrical aeration provides symmetrical vortices. PIV technique is found to be a useful tool to characterize the number of aeration modes through the time averaged surface plot of 30 dual frames in one second. Based on specified orifice plate configuration (orifice spacing is 27.5mm and orifice size of 1.6mm), PIV spatial resolution with orifice can be observed up to four at 10.4m/s gas velocity with a time interval of 1/60s for each frame.

Nomenclature

Symbol	Description	Unit
C	Concentration of particles	wt. %
D	Column diameter	m
d_o	Orifice diameter	m
ε_g	Overall gas holdup	dimensionless
ε_{max}	Maximum voidage during transition	dimensionless
f_o	Characteristic frequency	Hz
H	Static liquid height	m
H_o	Aerated liquid height	m
j	Drift-flux	m/s
q	Superficial gas velocity	m/s
q_{max}	Velocity at maximum voidage during transition regime	m/s
u	Actual gas phase rise velocity	m/s
$u(x,t)$	Fluctuating velocity	m/s
u	x component of fluctuating velocity	m/s
$U(x,t)$	Eulerian velocity	m/s
U_L	Superficial Liquid velocity	m/s
u'	r.m.s velocity	m/s
$u_o'(x)$	r.m.s. axial velocity	m/s

Greek symbols

Symbol	Description	Unit
φ	Free plate area ratio	%
ψ	Sphericity	dimensionless
ρ_G	Gas density	$kg.m^{-3}$
ρ_L	Liquid density	$kg.m^{-3}$
τ_o	Characteristic time	s
σ	Surface tension	N/m
σ_u	Standard deviation	m/s
μ_L	Liquid viscosity	mPa s

LIST OF FIGURES

LIST OF TABLES

CHAPTER 1 INTRODUCTION

1.1 Objectives and Scope

One of the goals of this research is to conduct a systematic study of the effect of solid type, size, concentration and liquid phase properties on the transition gas velocity (i.e. when maximum voidage occurred at transition regime) which is caused by the instability of flow regime when higher gas velocity is introduced. Another goal of this project is to access the possibility of using PIV (Particle Image Velocimetry) technique to measure the liquid velocity at transition regime. In that case, there is a comparison of liquid circulation and fluctuation velocity between simple bubble column and the column containing draught tube. As a result, liquid flow velocity can be interpreted for determination of transition regime in bubble columns.

Also, attempt will be made to obtain information regarding time averaged flow field of partial aeration using single to tetra orifices in a bubble column. The results from this study provide the information on the maximum applicability of PIV system resolution

The scope encompasses the following aspects of work:

1. identification of flow regime in a fully aerated bubble column;
2. investigation on the effect of solid concentration and viscosity on the transition regime (column dimension will be considered in this case);
3. identifying the liquid velocity distribution in the transition regime using PIV technique; Normal stresses and Reynolds stresses will be calculated;
4. studies on the liquid flow structure using partial aeration; the impact of orifice number; and

5. comparing the liquid flow pattern at partial aeration and uniform aeration using PIV technique.

1.2 Organization of thesis

This thesis is organized to address the study of hydrodynamics in two- and three-phase bubble column and column containing draught tube experimentally.

Chapter 1 introduces the objectives of this research and briefly describes the scope of upcoming chapters.

Chapter 2 reviews experimental research into the identification of flow regimes especially transition regime using multiple orifices. Important influencing factors on the transition regime will also be reviewed in this chapter. In addition, liquid phase behavior in bubble column and in airlift reactors will be discussed. Effect of gas distribution depending their placement on the liquid flow field will be introduced.

Chapter 3 describes the experimental apparatus used in this work. Measurement techniques, experimental conditions and procedures will also be summarized in this chapter. In addition, theoretical definition on Reynolds stress to understand the liquid fluctuation in the column will be specified.

Results and discussion are presented in Chapter 4. Viscosity and solid concentration factors influencing the flow regime transition will be described. Liquid velocity

distribution in bubble column with and without draught tube will be addressed. In addition, the comparison between single and multiple aeration of liquid flow pattern based on experimental results will be also addressed.

Conclusions from 1) the experimental study on flow regime transition by the effect of viscosity and particle loading 2) liquid flow pattern at the wall and their fluctuation velocity by Reynolds stresses 3) liquid flow pattern by different placement of aeration are summarized in chapter 5. Recommendations arising from this work include suggestions for further study.

CHAPTER 2 LITERATURE REVIEW

2.1 General

The air is dispersed at the bottom of a vertical column through properly single or multiorifice designed spargers and a gas plenum chamber, and it flows upwards through a column of liquid which is either stagnant or moving rather slowly and concurrently with the gas flow. This can be seen in the type of bubble column.

Knowledge of hydrodynamic behavior in a bubble column is very important for prediction of the design parameters, such as heat and mass transfer coefficients, critical suspension speed etc. The hydrodynamic behavior of bubble columns consists of the macroscopic or large-scale phenomena and the microscopic of local phenomena. The macroscopic flow phenomena include flow regimes, gas holdup, the gross liquid circulation (i.e. upflow of liquid in the column center and downflow along the column wall) etc. The microscopic flow phenomena are more likely to be associated with the gas phase including the bubble wake interaction with the continuous phase, bubble coalescence, and bubble breakup. Thus, in any reactor design or modeling of bubble columns, both the macroscopic and microscopic flow phenomena have to be taken into account.

2.1.1 Bubble columns and modified bubble columns

Bubble columns are used as reactors in which one or several gases are brought into contact and react with the liquid phase or a component suspended in it (Deckwer, 1992). The gas is dispersed from the bottom through the various types of distributors and liquid phase, may move cocurrent or counter-current with the flow of gas phase. Due to its simple construction and economically favorable, bubble columns are widely used.

Advantageous of these reactors include high rate of circulation due to rising bubble entrainment and any solids such as catalyst, reagent or biomass are uniformly distributed. High heat transfer coefficients therefore provide a uniform temperature throughout. But there may be some drawback to use simple type of bubble column, such as the short gas residence time due to rising bubbles and adverse effect of increased back mixing due to liquid circulation.

To compensate the drawback, modified bubble columns are adapted. Gas is bubbled in the tube region and the liquid flow upwards in the tube and downwards in the annulus by airlift action. These types of modified columns are widely used in various processes, such as chemical, fermentation, leaching and waste water treatment processes. Incorporation of additional perforated plates, multilayer appliances, induced fluid circulation systems etc. intensified mass transfer, reduces the fraction of large bubbles and prevents back-mixing in both phases. In addition, liquid circulation influences the gas holdup in the column, prevailing flow regime, heat and mass transfer coefficients and the extent of mixing characteristic.

2.1.2 Description of flow field in bubble column

The hydrodynamics (i.e. mixing characteristic, bubble size distribution, gas holdup etc.) of a bubble column is significantly affected by the flow regime prevailing in the bubble column. Ample evidence of this dependency is available in the literature (e.g. Zahradnik et al., 1997, Vial et al., 2001, Shnip et al., 1992, Sarrafi et al., 1999, etc.) and various criteria have been proposed by different researchers to delineate the flow regimes (Deckwer et al., 1980). They presented a flow regime map (see fig. 2.1.2) which qualitatively characterizes the dependence of flow regimes on column and superficial gas velocity. There is no heterogeneous regime observed until 0.15m/s gas velocity with the column size (0.15m) of present study. In column less than 0.1m in diameter, the large bubble may fill the entire column and form slugs; this is known as slug flow regime. In larger diameter column, large bubbles are formed without producing slugs. As these large bubbles rise through the column, there is an increase in turbulence; hence this is called churn-turbulent regime (heterogeneous regime). The shaded area in Fig. 2.1.2 indicates the transition region between various flow regimes. The exact boundaries associated with the transition regions will probably vary with the system studied.

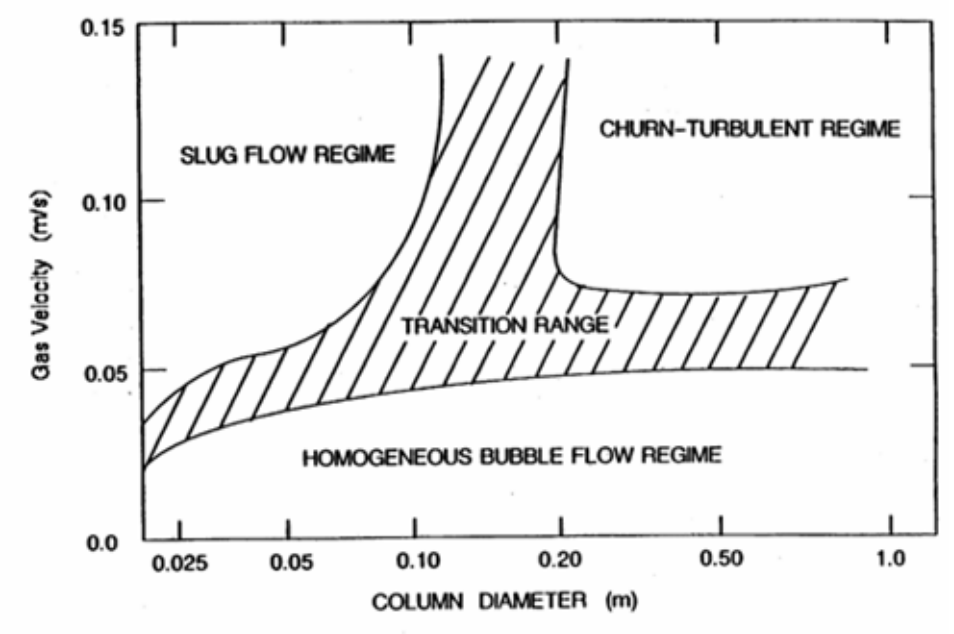

Fig.2.1.2 Bubble column flow regime map (adopted from Deckwer et al., 1980).

2.1.3 Flow regime

At low gas velocities ($0 < q < 0.05$m/s) discrete bubbles rise through the liquid phase in a straight chain and without interacting with each other. The bubbles are nearly spherical and uniform in size which is dependent upon the nature of the orifices in the sparger, and liquid phase properties. The bubble velocity is in the range 0.18-0.3 m/s for low viscosity systems (Saxena and Chen, 1994) and this regime is referred to as the homogeneous or discrete bubbling or quiescent regime. The gas holdup increases rapidly with an increase in superficial gas velocity.

As the gas velocity is further increased, bubble interaction sets in and larger coalesced bubbles are formed. The size range for the bubbles increases as this move upward the liquid moves downward to fill the gaps or voids. Thus liquid motion starts and better

liquid mixing is achieved with increasing gas velocity. This bubble coalescence regime is designated as the transition regime. The rate of increase of ε_g in this regime is smaller than in the homogeneous regime. This regime is usually obtained for gas velocities in the range $0.05 < q < 0.1$m/s, the transition from the homogeneous to the heterogeneous bubbling feature in the dispersion is also defined in terms of the drift-flux concept of Wallis, 1969. For batch operation, $q(1-\varepsilon_g)$ is plotted against ε_g and the change in slope is taken to indicate the transition from a homogeneous to a heterogeneous regime. Zuber and Findlay, 1965 have proposed to identify this transition in a plot of (q/ε_g) versus q where the slope change occurs. And, gas holdup was calculated by from visual observations of the expanded and static liquid height in the column. $\varepsilon_g = \frac{(H' - H)}{H}$ where H' is the aerated liquid height and H is the static liquid height. Present study will conduct with the drift flux analysis and measure the transition gas velocity at maximum voidage prevailed.

As the gas velocity is further increased, $q > 0.1$ m/s, the degree of bubble coalescence in the column increases and large bubbles coexisting with small bubbles are observed. The liquid mixing and turbulent agitation in the column are excessive. A wide bubble size distribution prevails, and large bubble rise through the central region of the bubble column. This regime is designated as the heterogeneous regime.

2.1.4 Methods of measurement

In the past, flow regimes used to be distinguished by visual observation. For experimental way to identify the flow pattern, the average gas holdup measurement is

the preferred way to characterize the dispersion (Zahardnik et al., 1997). Fig.2.1.4 (a) illustrates schematically gas voidage versus superficial gas velocity, q obtained in a bubble column. The homogeneous regime is characterized by the linearity of the curve from figure 2.1.4 (a) the fully developed heterogeneous regime is observed at higher q, starting from the point when the gas holdup exhibits a minimum. A plateau is observed in the transition reflecting the development of liquid macroscale circulation.

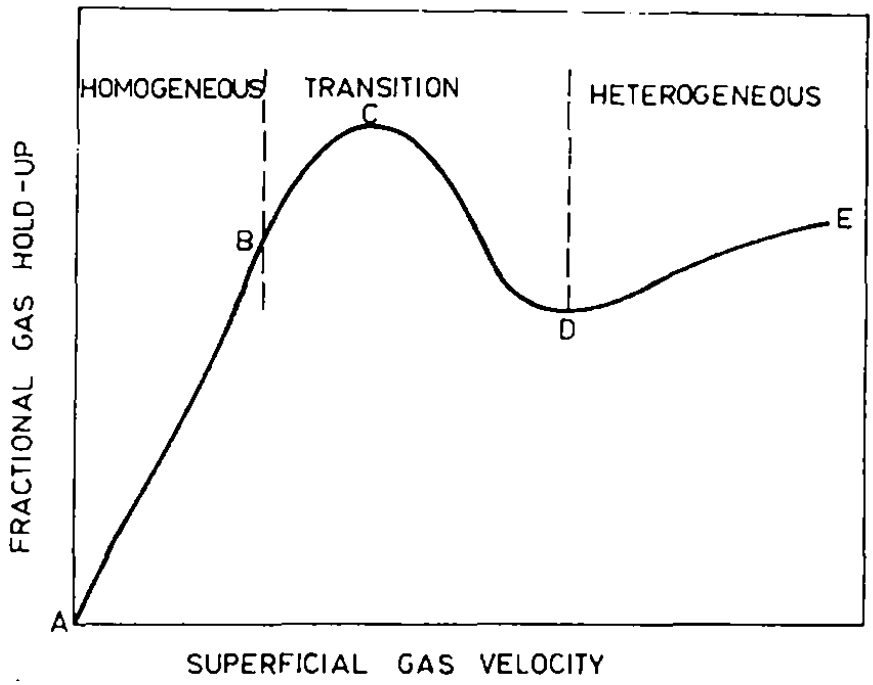

Fig.2.1.4 (a) Schematic representation of the gas holdup behaviour in the homogeneous, transition and heterogeneous bubbling regimes (adapted from Zahardnik et al., 1997).

Another way to describe regime with voidage is provided by the drift-flux analysis. It is plotted as q/ε_g vs $q+U_L$. A change in flow pattern shows by a change of slope of the curve. This is more suitable for the airlift reactors. In batch column, Wallis, 1969 plot the drift flux $q(1-\varepsilon_g)$ against gas holdup, ε_g. And drift flux is defined as the volumetric flux of gas relative to a surface moving at the average velocity of gas liquid flow systems.

Another method of regime identification is the dynamic gas disengagement technique (DGD). First the gas is fed into the column. The height of the dispersion was initially determined by visual observations. Then gas feed is shut off. The pressure transducer is connected to a few centimeters below the non-aerated liquid height. The measured disengagement profile (shown in Fig.2.1.4 (b)) enables the estimation of the holdup structure and allows the evaluation of the rise velocities of bubbles in the dispersion prior to gas flow interruption. DGD technique is not applicable in airlift reactors as the gas shut-off stops the liquid circulation.

Vial et al., 2001 a reported the theoretical analysis of the auto-correlation function of wall pressure fluctuations to study hydrodynamics. The model gives a characteristic time of the flow based on the pressure signal. This time is dependent on the hydrodynamic regime and the regime transition is characterized from the evolution of τ_o and f_o versus q.

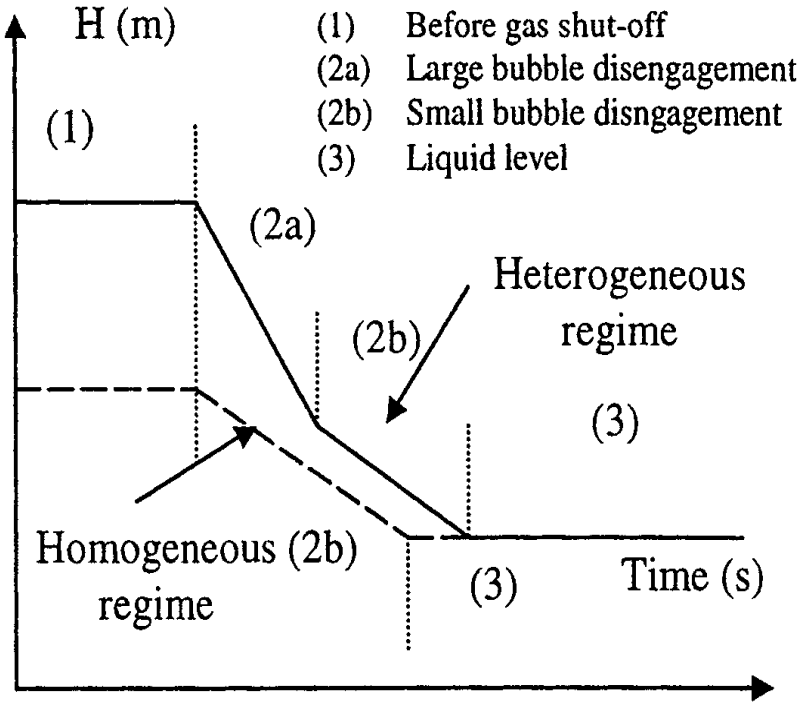

Figure 2.1.4 (b) Determination of regime transitions in bubble columns (adapted by Vial et al., 2001 a)

2.1.5 Flow regime transition

The knowledge of the transition between the homogeneous bubble flow and the churn-turbulent flow regimes is important for the design and operation of industrial reactors. The transition velocity depends on gas distributor design, physical properties of the phases, operating conditions, and column size. The flow regimes and the regime transition have been studied extensively under ambient conditions over the last three decades (Wallis, 1969; Shah & Deckwer, 1983; Shnip et al., 1992; Tsuchiya & Nakanishi, 1992; Zahradnik et al., 1997, Fialova et al., 2003). Most of these studies pointed out a critical role played by the liquid-phase turbulence during the regime

transition, and employed phenomenological models to predict the flow transition from the homogeneous regime to the heterogeneous regime.

2.2 Physical factors affecting flow regimes transition

2.2.2.1 Column dimension

A bubble column dimension on flow regime is also vital for scale up and design of real apparatus. These dimensions include D, diameter of bubble column, *H*, unaerated liquid height or so called column height, and A=*H*/D, aspect ratio. The diameter D should exceed 0.1–0.2 m (Jamialahmadi & Muller-Steinhagen, 1993) *H* should be larger than 1-3m (Wilkinson et al., 1992) and the aspect ratio A is recommended above 5 (Wilkinson et al., 1992; Zahradnik et al., 1997). The voidage decreases with D, *H* and A. However, the influence of column height on gas holdup is negligible for A > 5.

In bigger containers, the physical reason for the asymptotic fall of the voidage with the column size is the progressive development of vigorous liquid motions and turbulent circulations. The effect of D is often related to the turbulence scale (Zahradnik et al., 1997).

And the effect of *H* is related to the circulations (Jamialahmadi & Muller-Steinhagen, 1993). (Zahradnik et al., 1997) reported that their voidage data in the homogeneous range decreased with an increase of both *H* and D, However decrease in voidage data does not prove decrease in stability. But Sarrafi et al., 1999, reported that voidage

decrease with *H*, as expected, and an increase with D, as unexpected. Finally Ruzicka et al., 2001 b proved that the column size destabilizes the homogeneous regime. They suggest that the column aspect ratio, A=*H*/D alone cannot replace the simultaneous effect of the column height and width. We will investigate the liquid height effect in viscous liquid (Section 4.1).

2.2.2.2 Particle concentration

A third solid phase may be added which is dispersed continuously in the liquid phase by the bubble induced motion of the liquid. These solid particles may be very small or large in size and fine or coarse powder.

Many researchers have been conducted the solid loading in the bubble column on gas holdup (Jamialahmadi & Müller-Steinhagen, 1993 and ref: there in, Saxena & Chen, 1994; Garcia-Ochoa et al., 1997; Gentile et al., 2003). Increasing solid concentration, particle size and solid-liquid density difference results in a decrease in gas holdup. This trend is reversed if the particle size is below 10 μm. Addition of wettable and non-wettable has also different effect on gas holdup depending on the bubble coalescence rate.

The effect of particle concentration on the transition regime using small particles can be found in Krishna et al., 1999. In addition, the particle effect on macroscopic flow structure was studied by Tzeng et al., 1993, Lin et al., 1996. The vortex size, wavelength, frequency, and vortex descending velocity are changed due to increasing bubble coalescence rate. And changing to transition regime in the presence of solid

phase indicated by the wavelength levels off quicker. Due to the limitation of this measuring with particles, there is still lack of detailed understanding of transition regime, such as the particle size and density effect on the flow structure and the liquid phase properties in different operating conditions.

There have been very limited studies on the effect of solid on transition gas velocity in bubble columns. The addition of solids increased or decreased the transition gas velocity in experiments conducted in the batch mode of operation. This was explained by coalescence rate or bubble break up rate. Krishna et al., 1999 concluded that addition of catalyst particles enhanced the regime transition. They reported that it can be caused by increasing coalescence rate. The addition of particles to the liquid phase on the transition point is not able to predict by Reilly or Wilkinson correlations. In contrast, Chen et al., 1994 applied 0.5mm glass beads and 1.5mm acetate beads of 1-10% and concluded that the existence of solid phase does not exhibit significant influence on the transition under low solid holdups. Thus, to get more information about particle effects on transition, the present study will conduct the effect of particle concentration, size and density on the transition regime.

2.2.2.3 Distributor type

The gas phase plays a very important role in the design and operation of a bubble-column reactor and in determining the chemical conversion achieved. The design of gas sparger determines the uniformity of gas release across the bubble column reactor and the initial bubble size. Effect of distributor type on the gas holdup can be seen in Fig. 2.2.2.3 they also acknowledged that orifice diameter of 1.6mm cannot generate

the homogeneous regime and ≤ 1mm is recommended for homogeneous regime. Thus, to study the transition regime in the column of 0.15m diameter, φ = 0.2% of perforated plate with 0.5mm orifice is applied in the present study.

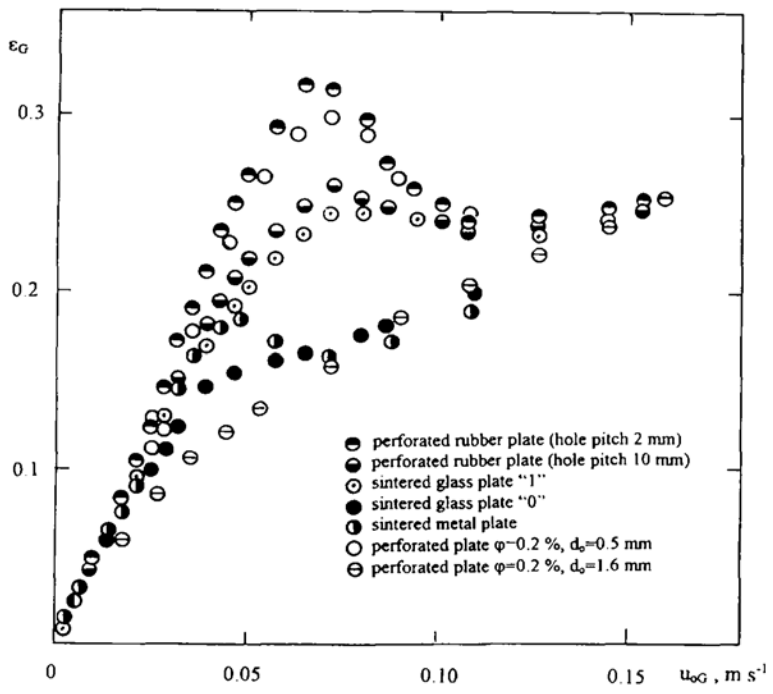

Fig. 2.2.2.3 The effect of distributor type on gas holdup; column diameter: 0.14 m, aspect ratio: 7 (adapted from Zahradnik et al., 1997).

Ruzicka et al., 2001a reported that the plates with small and closely spaced orifices produce uniform layers of equal-sized spherical bubbles at low flow rate. At high flow rate, the flow pattern change due to the instability of homogeneous regime and form transition. For the plates with large orifices, non uniform distribution was observed and only heterogeneous regime was obtained.

The gas sparger which is of utmost importance in conventional bubble columns has less influence for airlift reactors due to the dependency between the gas holdup and the liquid velocity (Wild et al., 2003).

2.2.2.4 Liquid phase properties

Liquid phase viscosity on the gas holdup was studied by Krishna 1997 & 2000. Reduction in the surface tension of the liquid led to a decrease in bubble stability and thus to smaller bubbles. This condition can be created by either adding surface active components to the liquid phase or using a liquid with a smaller value of surface tension. Similarly, an increase in liquid viscosity lowered the bubble break-up rates (Saxena and Chen, 1994). They reviewed that ε_g increases with viscosity ranging from 1cp to 3 cp and then decreases sharply till about 11cp and then decreases slowly up to about 39cp. The changes were relatively sharp at higher gas velocities. This was explained on the basis of the bubble coalescence phenomenon on liquid-phase viscosity. In the small viscosity range up to about 3cp, bubble coalescence was insignificant and moderate drag forces contributed to more uniform distribution of bubbles and to higher gas holdups. At higher viscosity values, bubble coalescence decreased the gas phase holdup. But the knowledge of viscosity effect on the transition regime in bubble column is not yet well understood.

Zahradnik et al., 1997 reported the viscosity of saccharose solution on the transition regime is found to be significant. Existence of drag forces promotes the bubble coalescence in the distributor region. They used the saccharose concentration starting from 30wt. % and this study will focus on the viscosity range 0-41wt. % of glucose at

different aspect ratio. Addition of alcohol to the liquid phase delays the transition point (Krishna et al., 1999, Zahradnik et al., 1997). It is likely to be caused by the enhancement of homogeneous regime stability. Thus, addition of surface active agent to viscous phase system is predicted to maintain the stability of homogeneous regime.

2.2.2.5 System pressure

The effect of the gas density or the operating pressure on gas holdup and flow regimes has been investigated by some authors (Idogawa et al., 1986, 1987; Kojima et al., 1997; Luo et al., 1999) for bubble columns and airlift reactors and correlations or models have been proposed at operating pressure values up to 15 MPa.

The effect of the operating pressure on the onset transition has been examined by many researchers in bubble columns (Clark, 1990; Krishna et al., 1991; Wilkinson et al., 1992; Reilly et al., 1994; Lin et al., 1999b), in three-phase fluidized beds (Luo et al., 1997a), and in slurry bubble columns (Clark, 1990). The transition from the homogeneous to the heterogeneous regimes is generally found to be delayed to higher gas velocities and the gas holdup increases when the gas density or the operating pressure increase, even if the increase of gas holdup is smaller in airlift reactors than in semibatch bubble columns, due to the increase of overall circulation velocity with pressure (Letzel and Stankiewicz, 1999 a & b).

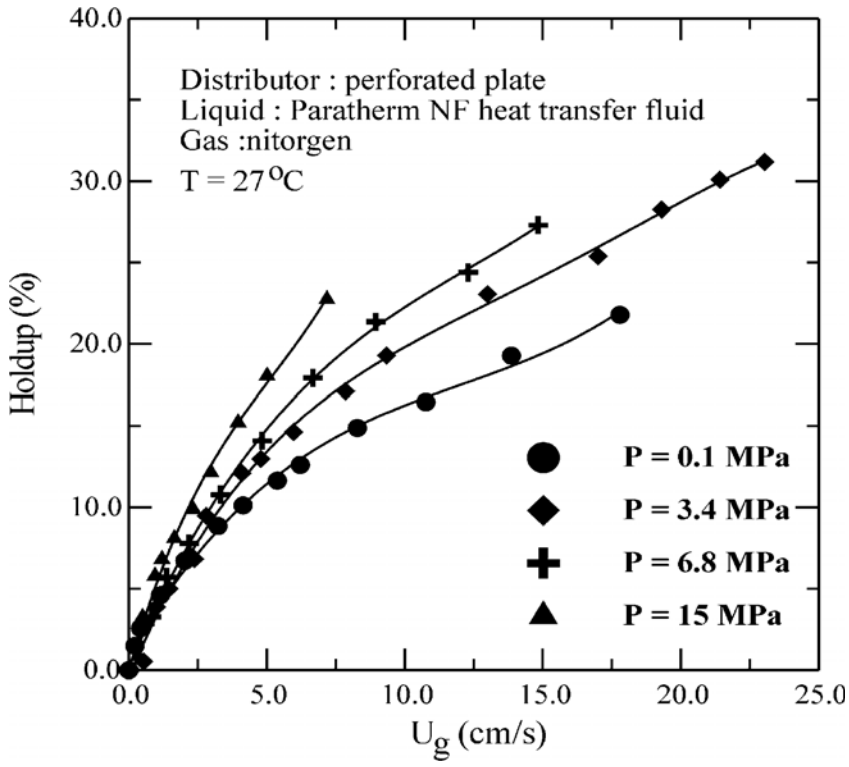

Fig. 2.2.2.5 Variation of gas holdup with respect to the superficial gas velocity for different operating pressure (adapted from Lin et al., 2001)

Increasing pressure or temperature delays the regime transition (Fan et al., 1999) and they showed that the rise velocity of single bubbles in liquids and liquid-solid suspensions decreases with an increase in pressure. Wilkinson et al., 1992, proposed a correlation to estimate the gas holdup and gas velocity at the transition point under high-pressure conditions. In general, the pressure effect on the flow regime transition is a result of the variation in bubble characteristics, such as bubble size and bubble size distribution (Wild et al., 2003). The bubble size and distribution are closely

associated with factors such as initial bubble size, bubble coalescence rates and bubble breakup rates. Under high-pressure conditions, bubble coalescence is suppressed and bubble breakup is enhanced. Wild also pointed out that the regime transition at high-pressure conditions in slurry bubble columns is still not fully understood, and further studies are needed to examine the effect of solids concentration on the transition velocity, to develop an accurate correlation, and to explore the transition mechanism.

2.3 Description of flow field in Column with Internal channel

The bubble column with draught tube is widely used in various processes, including chemical, fermentation, leaching and wastewater treatment processes (Onno et al., 2002). Gas and liquid can be introduced either into the annulus (Koide et al., 1983) creating cocurrent downflow pattern or into the draught tube (Koide et al., 1984) creating cocurrent upflow pattern in the draught tube. When the latter one is applied the system, the pressure difference provides the driving force for liquid circulation from the draught tube region to the annulus region. Column with internal channel consists of three flow regimes (I) no air bubbles (when liquid velocity in annulus is lower than slip velocity of bubbles in the liquid) (II) bubbles remain stationary (when liquid velocity in annulus is equal slip velocity of bubbles in the liquid) and (III) bubbles flow downwards and into the riser (when liquid velocity in annulus is higher than slip velocity of bubbles in the liquid) (van Benthum et al., 1999). There are the transitions between regimes I-II and II-III. Their study shows that transition from regime II to III was occurred at gas holdup of 10% and 12% by the reference they

mentioned. The present study will provide information on the Reynolds stresses at these regimes.

Wild et al., 2003 reviewed that in airlift reactors, no maximum of the gas holdup is observed, even with efficient gas distribution systems: this is due to the relation between the gas and the liquid velocity which have opposite effects on the gas holdup: an increasing gas velocity leads to an increase of the overall liquid velocity, which reduces in turn the increase of the gas holdup.

2.4. Measurement techniques for liquid flow velocities

The determination of local velocities in multiphase flows has been subject to experimental investigation for many years. Measurement principles for the determination of local liquid velocities in multiphase flows include optical, mechanical, thermal and mass transfer effects. In addition, measurement techniques can be divided into invasive and non-invasive methods. Among the optical methods, Laser Doppler Anemometry (LDA) has been a standard widely accepted in multiphase research. As a non-invasive optical measurement technique, LDA is based on the Doppler signals induced by liquid flowing through a control volume generated by two intersecting Laser beams (Crowe et al., 1998). Main advantage of this method is the complete absence of flow disturbance during measurements; most serious downside is the fact that no measurements can be performed in opaque media or when particles or more than very little gas content is present.

Another optical, non-invasive method which not only can determine liquid velocities but also covers bubble or particle motions is known as Particle Image Velocimetry (PIV) (Lindken et al., 1999). Seeding particles are added to the liquid and the motions of which can be traced with high speed video cameras. In comparison to LDA, the control volume for this method is rather large; the video camera delivers images from a light sheet that has to be projected into the liquid by means of an oscillating Laser beam. Full three-dimensional flow vectors can be obtained. It is also possible to visualize the liquid motion in the wake of a rising bubble at high local and temporal resolution by means of a special phase masking method (Br¨ucker, 1996, Lindken et al., 1999). As with the LDA, this method delivers interesting results for the fine-scale bubble flow phenomena but is not viable at high gas holdups.

2.4.1.1 Liquid velocity field measurement in bubble column

Gas-liquid system has been studied by LDA (Mudde et al., 1997 a & b, Vial et al., 2001 b, Olmos et al., 2003) and by PIV (Reese and Fan, 1994) to observe the flow structure in bubble columns. Among them, Vial et al., 2001 b studied the liquid phase behaviour caused by gas distribution and transition regime. The measurement was done under 15-20% gas holdup. They reported that transition was characterized by local liquid recirculation near the wall where the mean liquid velocity is negative. High positive values can be measured at the center of the column. Using PIV to study flow regimes (Fig. 2.4.1.1) in two and three phase bubble column can be found in limited literature because there are some limitation to use with this technique, the gas holdup should be <4%, and only two phase system can be applied. However, Chen & Fan, 1992, Chen et al., 1994, Lin et al., 1996, Tzeng et al., 1993 applied this technique

to study the hydrodynamics in three-dimensional gas-liquid-solid systems combining refractive index matching technique in order the particles not to be seen.

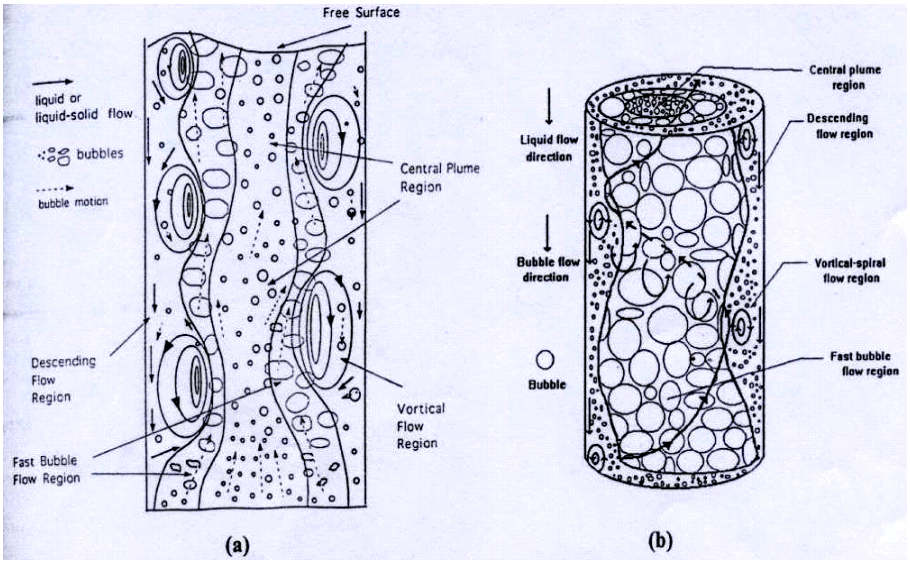

Figure 2.4.1.1 Classification of regions accounting for the macroscopic flow structures: (a) 2-D bubble column (Tzeng et al., 1993); (b) 3-D bubble column (Chen et al., 1994) (adapted from Lin et al., 1996).

Recently, Olmos et al., 2003 measured the liquid velocity at different flow regimes in bubble column near the wall using LDA technique. The gas holdup was applied upto 25% so that the measurement was only possible for the wall region. The magnitude of horizontal normal stress was found twice that of vertical normal stresses. The effect of gas distributor on the flow regime was significant. Thus, in this kind of operating condition, the liquid flow measurement by PIV at wall region will be challenging task as well as comparable to the results obtained by LDA. In addition, the flow structure in the absence or presence of draught tube system is extended in this present work.

2.4.1.2 Liquid flow velocity in airlift reactors

In airlift reactors, the liquid circulation is induced by the hydrostatic unequilibrium caused by the density difference between the riser where the gas is injected and the downcomer. The liquid velocities are generally higher than in bubble columns, especially in the case of external loop airlift reactors for which the range may be one to two orders of magnitude higher (Wild et al., 2003). The global circulation velocity is affected by various design and operating parameters such as the cross-sectional area ratio of downcomer to riser, the height to diameter ratio, the gas velocity, the properties of the phases etc. (Dhaouadi et al., 1997). Lin et al., 2003 recently analyzed on the flow fields in airlift reactor.

2.4.1.3 Velocity fluctuation and Reynolds stresses

Reynolds stresses are encountered in describing single phase turbulent flows. However, to determine the liquid velocity field with multiple orifice systems, the high evolution of gas holdup is needed to be considered. Reynolds stresses are defined to be interpreted as the turbulent fluctuation in the liquid phase in addition to the motion of the dispersed particles (Mudde et al., 1997a). Therefore, Reynolds stresses are applied to the system to study the flow regime in the bubble column reactors. Horizontal normal stress found to peak in the center whereas vertical normal stress peaks close to the wall due to the swinging motion of the central bubble stream (Mudde et al., 1997 a). In addition, they acknowledged that the dominance of vortical structure can change the above phenomena to opposite effect. The analysis on the

high frequency content of normal stresses, i.e. turbulence, is an order of magnitude higher than bubble-induced normal stresses. Similarly, shear stress in the Reynolds stresses, the stress due to small scale shear-induced vorticity is higher than that of bubble-induced stress. But how the phenomena are like for partial aeration is questionable.

2.4.1.4 Flow pattern in bubble column at transition regime

Vial et al., 2001 b specified the transition regime using three different spargers. Transition regime is identified by circulation pattern with steep profiles and higher values of the local liquid velocity. And vortical-spiral structure occurred in this regime (Chen et al., 1994). The ratio between tangential mean velocity and axial value is the highest in the transition regime whereas the lowest are obtained when the heterogeneous regime is established. They explained it as the upward movement of bubbles disappeared when heterogeneous conditions prevail. Thus, their prediction on the time-averaged wall shear stress is higher in the transition regime due to the higher liquid value near the wall than those when heterogeneous regime occurred. Time averaged wall shear stress at transition regime using PIV will be discussed in the present work.

2.4.1.5 Effect of distributor placement on liquid circulation cell

Different aspect ratio and placement of distributor influence on the flow structure (Tzeng et al., 1993, Becker et al., 1994, Borchers et al., 1999, Becker et al., 1999, Deen et al., 2000). In a shallow column when the air is injected from the central part

of the column, the "gulf stream" phenomena and a pair of symmetrical liquid circulation cells are found.

Becker et al., 1994 measured the flow pattern with laser Doppler anemometry (LDA) in the case of a decentralized gas inlet, for a number of different aspect ratios and gas flow rates. The gas inlet was placed at the left of column. They found that the lower part of the bubble plume was stationary at low gas flow rates and directed to the left wall, under the influence of a large liquid vortex on the right hand side. The upper part of the bubble plume was meandering in a quasi-periodic way. For high gas rates the meandering behaviour was not observed. So the effect of different number of orifice and placement of them on the flow using PIV technique is an interesting subject for part of this work. In addition, more work on the investigation of whole field velocity data with high spatial and temporal resolution is necessary to obtain new experimental information about the flow fields of interest.

Experiments of the flow of a bubble plume in a 3-D bubble column were performed by Deen et al., 2000. The aspect ratio was 3 and a meandering plume was observed. The bubble plume in 3-D was likely to be moving randomly compared to 2-D column. They have done the measurement on the core region only. Wall region measurement is supplied by this work to get more information on this partial aeration. Wall and center fluctuation due to this single to tetra aeration will be discussed. Since the entrance region is likely to be influenced by the gas inlet, it is specifically investigated the velocity fluctuation on the entrance of the column.

2.5 Summary

Onset transition velocity in a bubble column has been extensively studied in recent decades. Physical factors including column dimensions, system pressure, liquid phase properties and solid concentration could have influence on the hydrodynamics of bubble column. This chapter reviews all these physical factors by evaluating related literature focusing on these parameters.

In addition, this review also concerns liquid flow field due to the gas distribution and flow regimes using PIV technique. Very limited studies on the liquid flow velocity and velocity fluctuation by transition regime also reviewed. Using PIV with refractive index matching techniques was found to observe the liquid flow of three-phase flow in bubble column.

Finally, placement of gas distribution on the liquid was found to affect the changes of vortex structures in the column.

CHAPTER 3 MATERIALS AND METHODS

The experimental apparatus was set up for the measurement of (a) $q_{\max}$, transition velocity at maximum voidage occurred (b) liquid flow field at $q_{\max}$ and (c) liquid velocity of single or partial aeration.

There are three sections in Chap.3. Section 3.1 represents the essential apparatus used in this work to study the flow regime. Descriptions for Particle Image Velocimetry (PIV) technique will be included in section 3.2. Finally, to study the performance of single to fourth orifice aeration, another type of orifice plate configuration will be mentioned in section 3.3.

3.1 Experimental setup and procedures for flow regime measurement

3.1.1 Bubble column setup

Fig. 3.1.1a represents the schematic diagram of the experimental apparatus showing (1) compressor, (2) pressure regulator, (3) flow meter, (4) gas chamber, (5) perforated plate, (6) Plexiglas® flat column, (7) drain valve, (8) *H*, static liquid height and (9) measuring tape. The open air system bubble column of 1.2m height, 0.15m square area was designed. Perforated plate was made of 3mm thick Plexiglas® and was put on the gas chamber. Orifice diameter used was 0.5mm and the 225 holes of the distributor were oriented in square pitch and the pitch distance was 10mm. Air from the compressor is passed through the gas regulator which is set at 60psi, is introduced to the gas chamber. Tap water ($\rho_L = 1000 Kg/m^3, \sigma = 0.07 N/m$) was used for solid

loading measurement and the experiments were done at room temperature. For viscosity measurement, deionized water was used.

3.1.1a Bubble column

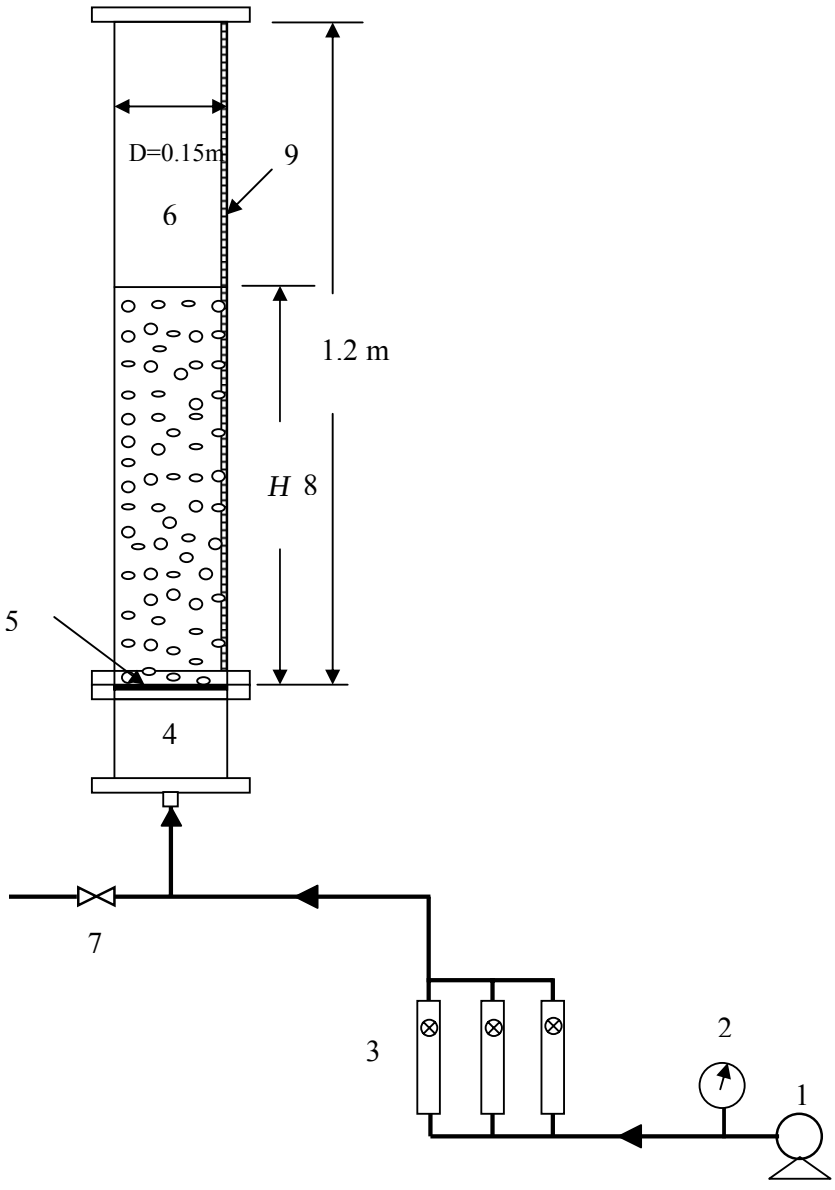

Figure 3.1.1a Schematic diagram of experimental bubble column

For the three phase system, low density polycarbonate particles, high density glass beads and glass beads were tested (Table 3.1). The air flow rate was read from the rotameters and the voidage was determined by the bed expansion. In order to stabilize the fluctuation of the air pressure, 2mins waiting time was allowed before changing another gas flow rate. The liquid was neither fed nor discharged.

a. Glucose measurement procedure

Glucose suspension was carried out as followed by the procedure; powder glucose was added to a small container of de-ionized water and was mixed with a stirrer. The resulting mixture was then added to the bubble column partially filled with de-ionized water. Additional water was added to fill the column to a certain height not including the volume of glucose amount added (0.15m diameter column). Experiments of liquid phase effect were initiated with specific volume. The column was then operated at a high gas flow rate for approximately 20minutes to ensure glucose was well mixed throughout the column. The gas flow rate was reduced to the lowest level of interest to start the data collection and increased gradually for additional data points. Then the voidage can be calculated from static pressure difference.

b. Solid loading measurement procedure

1. Particles were washed with tap water and then dried.
2. Weight the particles of different solid concentration.
3. Add in the water and increase the gas flow rate gradually for additional data points.

4. After each flow rate, read the changes of aerated liquid height which is the combination of solid, liquid and gas. That is called H'.
5. Calculate the gas voidage from the following equation.
6. Then draw the curve of $q(1-\varepsilon_g)$ vs ε_g or q vs ε_g as shown in Fig.3.1.1b. From that we can obtain the q_{max} .

The gas holdup is obtained by $\varepsilon_g = \frac{(H'-H)}{H}$ where H' and H are the aerated and static liquid heights respectively for two and three phase bubble column. Fig.3.1.1b represents the characterization of flow regime transition in the bubble column. Present study only conducts on the gas flow at maximum voidage during transition. We can determine q_{max} directly from the plot of $q(1-\varepsilon_g)$ vs ε_g.

TABLE 3.1 PHYSICAL PROPERTIES OF THE PARTICLES

Type of material	Mean diameter (μm)	Sphericity $\psi = \frac{A_{sphere}}{A_{particle}}$ (Hartman, et al. 1994)	Density (kg/m^3)
Polycarbonate	3000	0.75	1200
Glass sphere	500	1	2500
Glass sphere	3000	1	2500

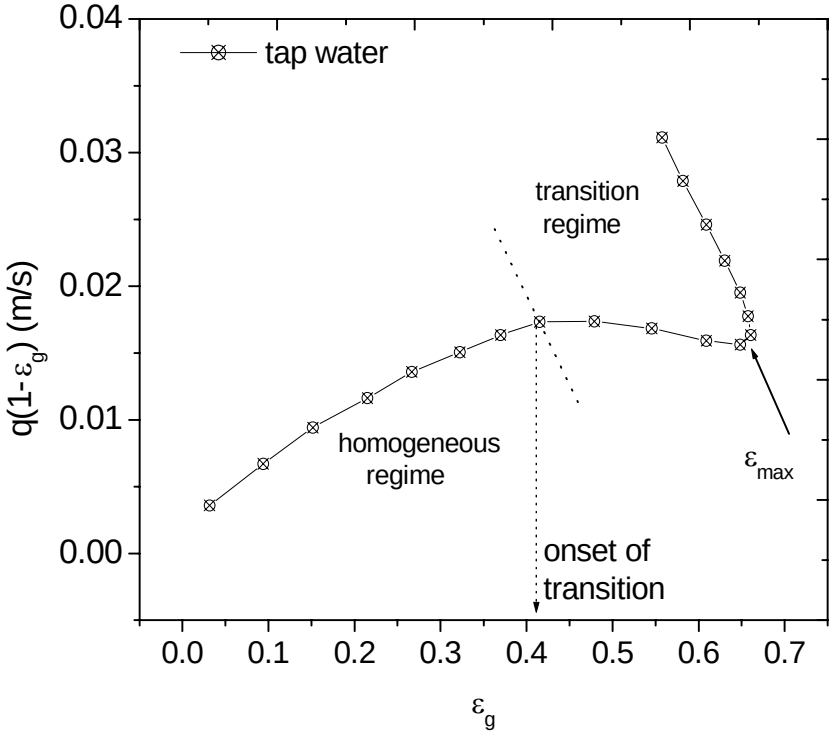

Figure 3.1.1b: Identification of flow regime in air-water system using drift flux model, D = 0.15m, *H*/D = 3.7; plate parameters: $\varphi = 0.2\%$, $d_o = 0.5$mm.

3.1.2 Orifice plate configuration

When the gases are fed in the column through the distributor, perforated plate is provided to speed up the gas distribution stage. Figure 3.1.2 shows perforated plate used in this work. There are 225 orifices contained for the measurement of (a). With this type of Plexiglas plate with a diameter of 0.5mm, the three flow regimes can be observed.

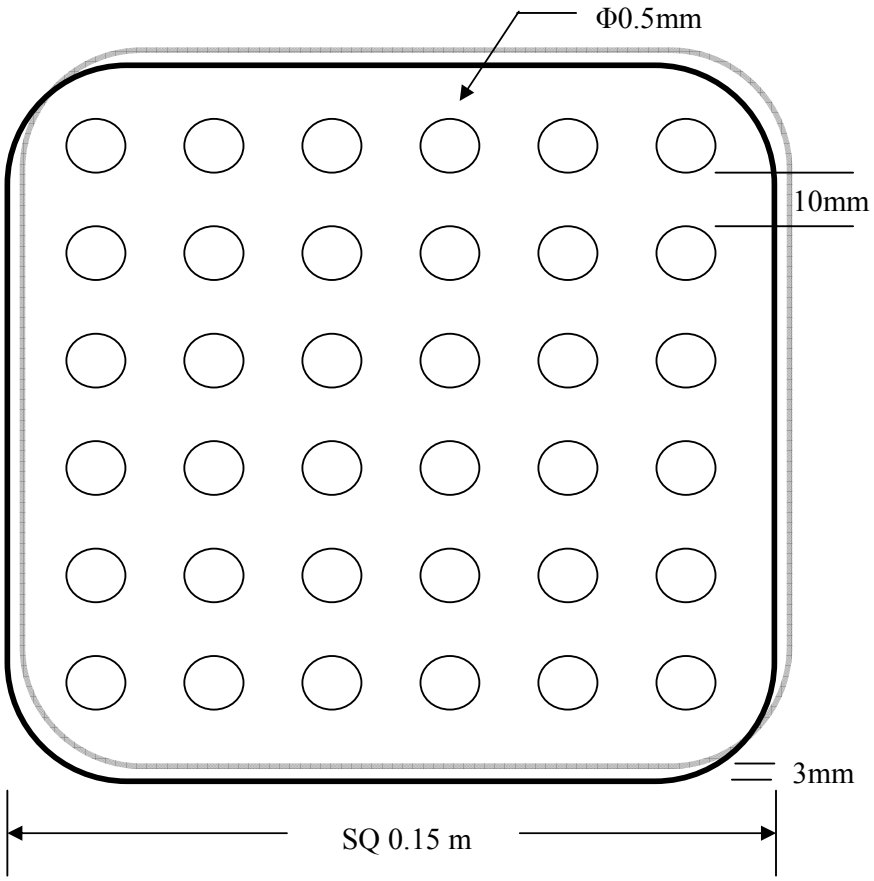

Figure 3.1.2: Schematic representation of the perforated plate distributor, orifice spacing = 10mm, plate thickness = 3mm, orifice diameter = 0.5mm, number of orifice = 225.

3.2 Method of PIV

Particle Image Velocimetry technique (PIV) can be considered one of the most important achievements of flow diagnostic technologies in the modern history of fluid mechanics. The technique recovers the instantaneous two- and three-dimensional velocity vector fields from multiple photographic images of a particle field within a plane or volumetric slab of a seeded flow, which is illuminated by a light source. The velocity field of both phases can be obtained by dividing the measured displacements by the exposure time delay Δt.

3.2.1.1 Measurement technique

A very powerful method to obtain quantitative information on the instantaneous structure of the flow is Particle Image Velocimetry (PIV).

PIV system includes the following:

- Laser and lightsheet optics
- Image capture component
- Synchronizer
- Analysis components-computer hardware and software
- Image shifting component

3.2.1.2 Calibration

Before velocity measurement is taken, the image of ruler, which is placed where laser is illuminated, is captured (can be seen Figure 3.2.1.1). Then the image scale (pixel) can be changed to real measurement scale of μm. Then we can proceed to take frame images and can analyze as the following steps.

Figure 3.2.1.1: Image taken for calibration to obtain real measurement from image measurement scale, (x, y) where x is horizontal direction, y is vertical direction.

The images were captured by PowerView^{TM} 4M 2K x 2K camera which is connected to LaserPulse^{TM} Computer Controlled Synchronizer. For liquid flow measurement, the colour filter is put in front of the camera to separate the liquid from the bubbles. The filter allows the light from the dye particle and avoids capturing the laser light.

Rhodamine B is used for this work, because its absorption spectrum (460-590 nm, max=550 nm) closely matches the available laser light wavelength (532 nm) and its emission spectrum (550-680 nm, max=590 nm) is almost completely separate from the laser light.

There are five basic procedures to obtain a complete PIV experiment. These steps are as follows:

1. seeding of the flow
2. illumination of cross section of the flow
3. recording of scatterers in the flow field
4. processing of the records
5. analysis for presentation

3.2.1.3 Reynolds stresses definitions

The Reynolds stresses $\langle u_i u_j \rangle$ play an important role in the equations for the mean velocity field. To understand the fluctuation of liquid turbulent in high gas fraction, the equations from table 3.2.1.3 will be applied for Reynolds stresses identification. u and v are horizontal and vertical component of velocity and x and y are the horizontal and vertical coordinates. Profiles are calculated by dividing the field of view into horizontal strips with a specified width. The averaged of the velocity components and the various Reynolds stresses for all fields for each strip are therefore calculated as in table 3.2.1.3. In other word, the data *i* from every frames of specific y with horizontal position x variable to the column width are summed and are divided by *N* (30 frames).

Table 3.2.1.3 Equations for Obtaining the Averaged Velocities and stresses (Ref: Mudde et. al., 1997)

Averaged horizontal velocity	$\langle u(i)\rangle = \frac{1}{N(i)} \sum_{\{x,y\}\in strip(i)} u(x,y)$	(1)
Averaged vertical velocity	$\langle v(i)\rangle = \frac{1}{N(i)} \sum_{\{x,y\}\in strip(i)} v(x,y)$	(2)
Horizontal normal stress	$\langle u'u'\rangle(i) = \left[\frac{1}{N(i)} \sum_{\{x,y\}\in strip(i)} u(x,y)u(x,y)\right] - (\langle u(i)\rangle)^2$	(3)
Vertical normal stress	$\langle v'v'\rangle(i) = \left[\frac{1}{N(i)} \sum_{\{x,y\}\in strip(i)} v(x,y)v(x,y)\right] - (\langle v(i)\rangle)^2$	(4)
Shear stress	$\langle u'v'\rangle(i) = \left[\frac{1}{N(i)} \sum_{\{x,y\}\in strip(i)} \{u(x,y) - \langle u(i)\rangle\}\{v(x,y) - \langle v(i)\rangle\}\right]$	(5)

With $N(i)$ the number of vectors in strip *i* (range of 1000-2500)

3.3 Experimental Set up and procedure for uniform aeration

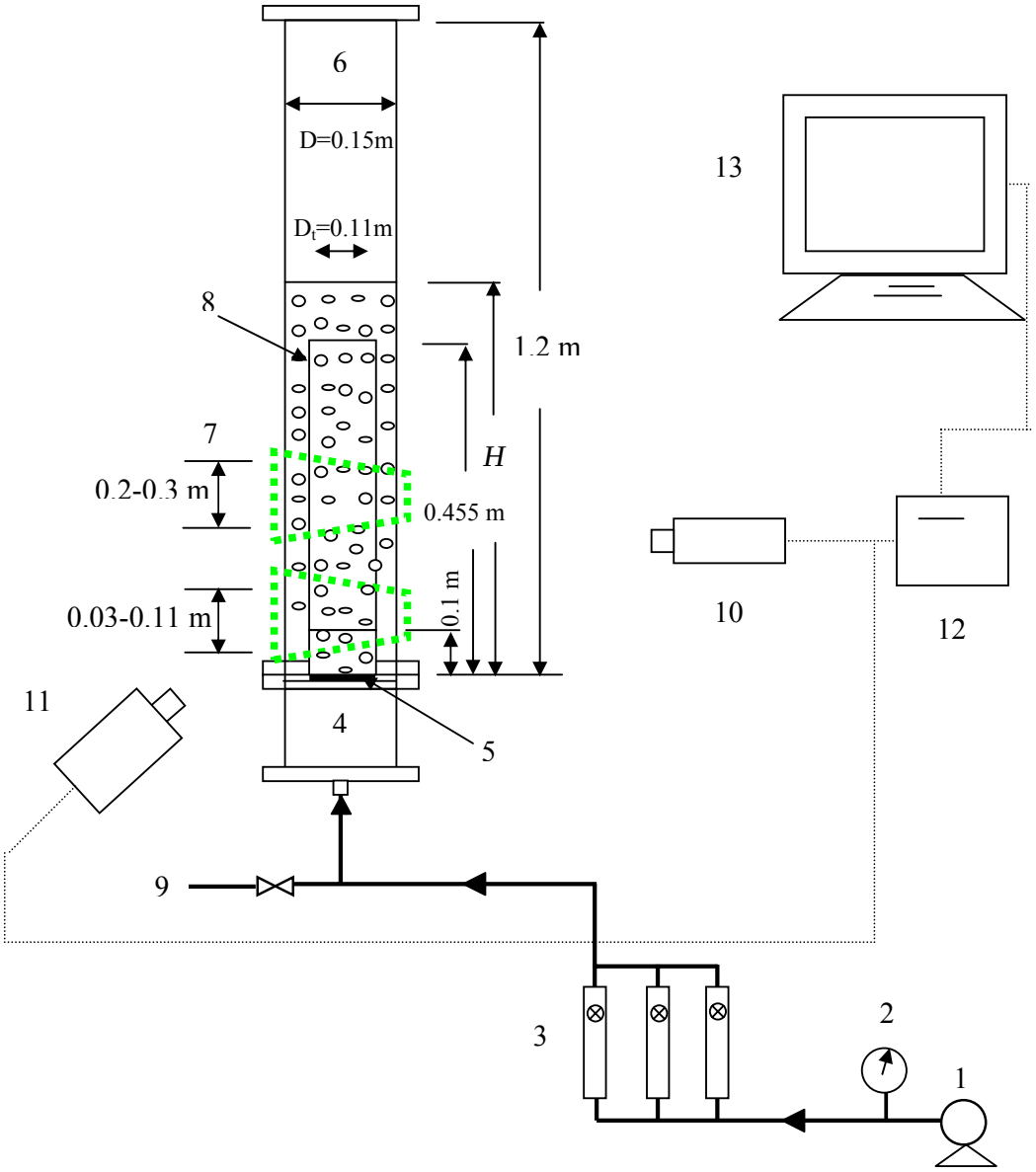

Figure 3.3.1.1: Schematic diagram of bubble column with draught tube showing the field of view for the testing zone of WDT and DT columns.

1. Air compressor
2. Pressure regulator
3. Flow meters
4. Gas chamber
5. Perforated plate
6. Bubble column
7. Test sections
8. draught tube
9. Drain valve
10. CCD camera
11. Laser generator
12. Synchronizer
13. Processing computer

3.3.1.1 Bubble column setup

Figure 3.3.1.1 shows the schematic diagram of bubble column. It consisted of a (1) compressor, (2) pressure regulator, (3) flow meter, (4) gas chamber, (5) perforated plate, (6) Plexiglas® flat column, (7) drain valve, (8) draught tube and include the whole PIV apparatus. The open air system bubble column of 1.2m height, 0.15m square area was designed. Perforated plate was made of 3mm thick Plexiglas® with pitch 10mm and was put on the gas chamber. Orifice diameter used was 0.5mm and the 49 holes of the distributor were oriented in square pitch and the pitch distance was 10mm. The draught tube (Figure 3.3.1.2) inside the column was 0.455m height. The bottom of the draught tube was 0.1m height far away from the bottom of the column. The annular space was 0.02m. The water is filled in the column up to 0.55m height so that the liquid can circulate from the top to the annular region until bottom of the column. Two test sections were measured at bottom y =0.03-0.11m and middle part y =0.2-0.3m of the column to obtain the flow field in the column without draught tube. The measurement was repeated for column with draught tube. The pressure used in this system was atmospheric pressure.

Laser Induced Fluorescence (LIF) method (Honkanen et al., 2002) was applied. Dyed polymer beads of 20-40μm methyl methacrylate with Rhodamine-B were used as fluorescent tracer particles. The color filter was attached to the CCD camera to detect the particles in the continuous phase. 30 image pairs were recorded at near the wall when the gas was introduced at critical value of superficial gas velocity for transition in the bubble column with and without draught tube.

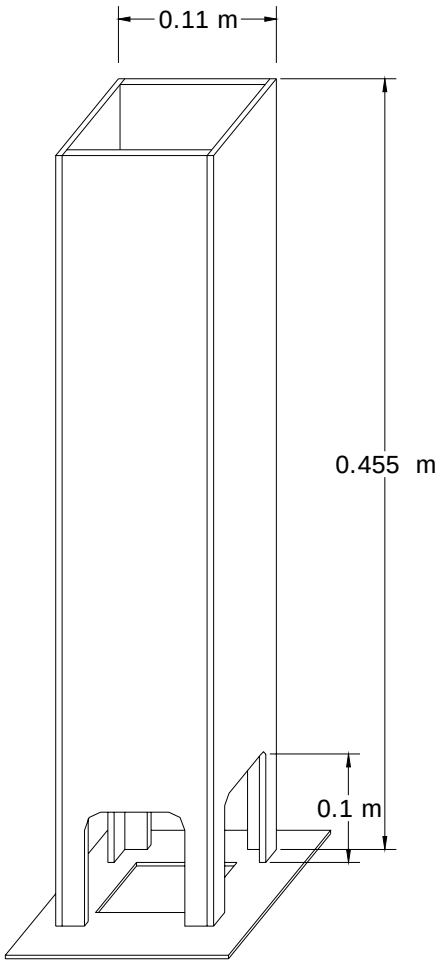

Figure 3.3.1.2: 3D-Schematic diameter of draught tub

3.3.1.2 Draught tube setup

The draught tube (draft tube) is made of Plexiglas which has the height of 0.455m long. The water is filled over this height and so the liquid can circulate well in the annulus region. The annulus space is 0.02m wide. The orifice plate is put on the gas chamber which is in the same position in the column without draught tube. The field of view for test section in Fig.3.3.1.1 and the schematic diameter of draught tube in Fig.3.3.1.2 can be seen.

3.4 Experimental conditions and procedures for partial aeration

This configuration of plate type is suitable for the pure heterogeneous regime. The orifice diameter and spacing is favorable for this regime only. Three orifice conditions were applied, (a) one orifice, 1 (b) two orifice, (1, 2) and (c) four orifice (1, 2, 3, 4).

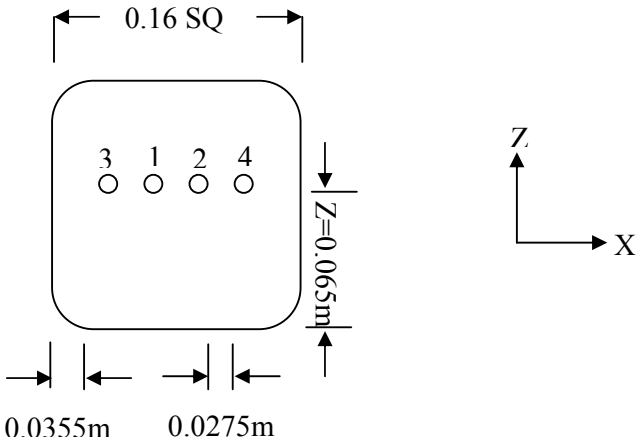

Figure 3.4 a: Design of orifice plate from the top view. Orifice spacing = 0.0275m, plate thickness = 3mm, orifice diameter = 1.6mm, number of orifice = 4.

Three test sections at bottom, y=0.03-0.11 m, middle, y=0.11-0.21 m, top, y=0.21-0.26 m were investigated. Measurement was made by three X-Y plane at Z = 0.065m (orifice region) and at Z = close to wall (wall region). The static liquid height used was 0.25 m. The exposure time delay is 200-2000 μs. The bubble column is the same as Figure 3.1.1 for all experiments. Only the orifice plate configuration is changed.

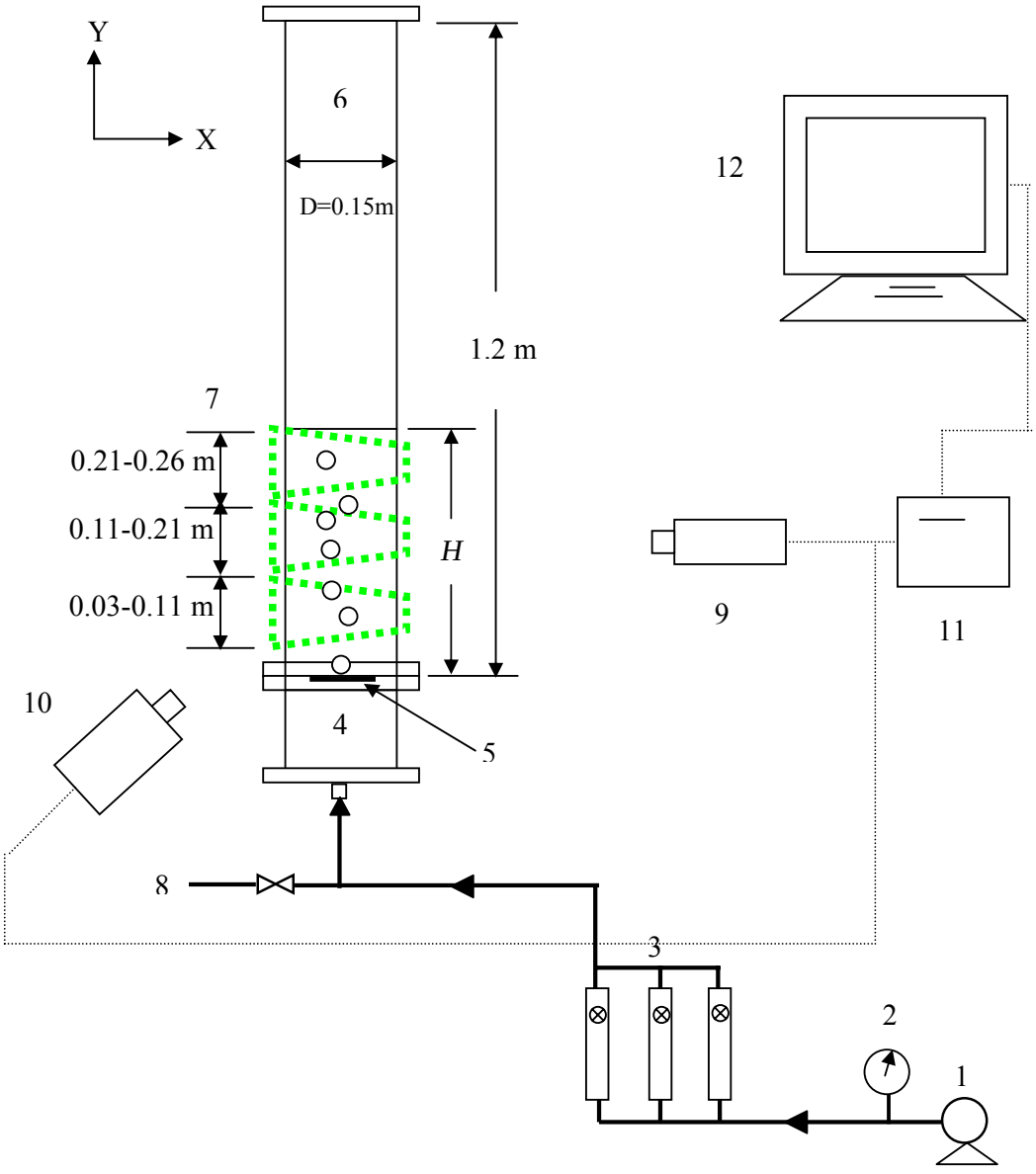

Figure 3.4 b: The field of view for three testing zones at z = 0.065 m in a partially aerated column.

CHAPTER 4 RESULTS AND DISCUSSION

Many works have been done on the critical value for transition which is the onset transition and different correlations have been done on the basis of drift flux model. But Vial et al., 2001 argued that there is a lack of accuracy due to the smallish difference between slopes when onset transition occurs. However, small column with small orifice size can give maximum peak forming during transition occurred and so the transition velocity is precisely obtained from drift-flux versus gas holdup plot. Effect of liquid phase properties and solid concentration with different size and density on $q_{\max}$ which is the transition velocity at maximum voidage will be discussed in section 4.1 and 4.2. And in the section 4.3 to 4.5, the liquid phase velocity near the wall of the column at $q_{\max}$, liquid velocity fluctuation and centerline liquid motion at that point will be discussed. Due to the limitation of PIV, liquid velocity studies can only conduct on two phase air-pure water system at low gas holdup. But attempt has been made at high gas holdup < 25% and measured at wall region in the present study.

In section 4.6, partially aerated system will be performed. Based on single to tetra aeration, effect of placement of gas inlet and number of orifice on liquid velocity and velocity fluctuation will be investigated.

4.1 Effect of liquid phase properties on the transition regime

Figure 4.1a shows the drift-flux profiles for solutions with different glucose concentrations. Glucose concentrations between 3.2 and 41wt. % with the range of apparent viscosities from 1.2 to 6.7mPa s were used (Table 4.1). It is found that gas holdup generally decreases with increasing viscosity as expected.

The value of ε_g corresponding to $q_{\max}$, the maximum gas superficial velocity corresponding to maximum gas voidage in the transition regime, decreased with increasing liquid viscosity, showing a narrowing of the homogeneous regime at high viscosities. Beyond about 4mPa s, the bubbling was in the heterogeneous regime for all superficial gas velocities, and no value of $q_{\max}$ was measurable. Zahradnik et al. (1997) also found that the homogeneous bubbling column was suppressed at high liquid viscosities. They observed that $\mu_L \geq$ 8mPa s suppressed the formation of homogeneous bubble beds. It seems that the pressure in present system was a bit higher so the flow pattern instability formed earlier. The gas holdup and bubble frequency increased and the bubble diameter decreased with increasing pressure (Idogawa et al., 1986). As a result, the population of bubble tends to disturb the flow stability.

Figure 4.1b shows the values of $q_{\max}$ due to the effect of solution viscosity for columns with different aspect ratios. It is clear that earlier transition was observed with increasing viscosity up to 3.5 mPa s. At a high viscosity, shear stresses between the liquid and bubble phase are higher. Bubbles remain in the liquid for a longer time, and this in turn enhances the possibility of bubble coalescence and fluctuation of fluid

flow patterns. Thus, higher viscosity promotes the transition from homogeneous towards heterogeneous flow by increasing the instability of the flow regime. Another explanation for earlier transition is caused by the formation of small bubbles at the gas distributor at high viscosity because of the increasing surface tension and reducing inertia force. The results also show that increasing the height to diameter aspect ratio caused earlier transition for the range of viscosities studied. Jamialahmadi and Muller-Steinhagen (1993) and Wilkinson et al. (1992) observed that a higher column height to diameter ratio increases the gas holdup due to the better liquid circulation. Ruzicka et al. (2001b) and Sarrafi et al. (1999) also found that the gas velocity for transition decreased with column size.

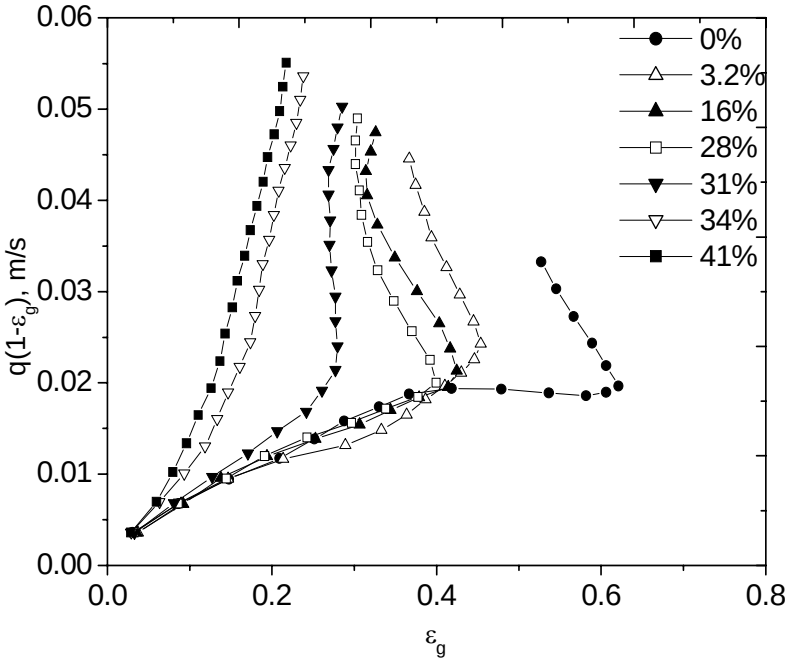

Figure 4.1 a: effect of glucose concentration on stability of homogeneous bubbling regime; D = 0.15m, H /D = 3.7; plate parameters: φ = 0.2%, d_o = 0.5mm.

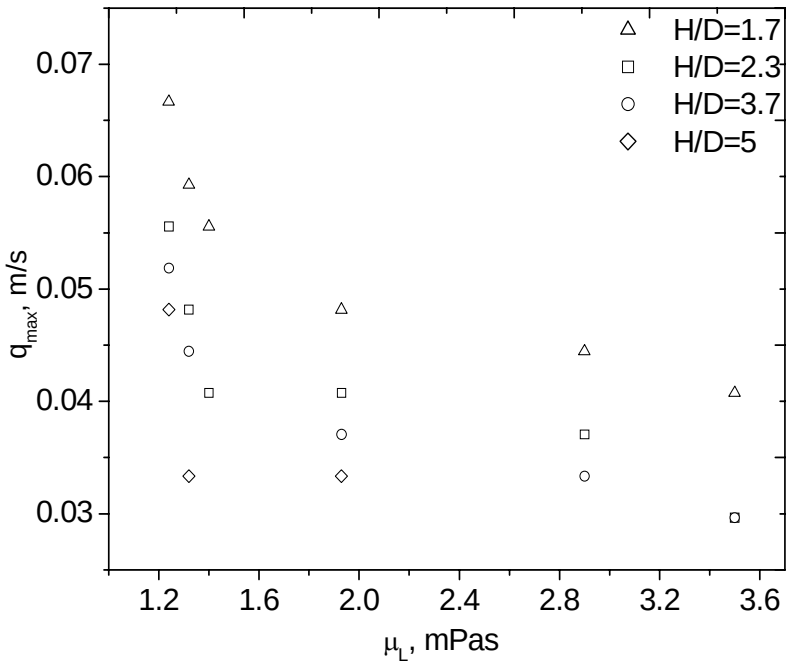

Figure 4.1 b: Profile of transition velocity versus viscosity at different aspect ratio. D = 0.15m, *H* /D = 1.7, 2.3, 3.7 & 5; plate parameters: φ = 0.2%, d_o = 0.5mm.

TABLE 4.1: APPARENT VISCOSITY DATA FOR GLUCOSE-DEIONIZED WATER

Table 4.1. Apparent viscosity data for glucose-deionized water

Mass fraction (% wt.)	Viscosity (mPa s)
0	1.24
0.032	1.32
0.061	1.4
0.163	1.93
0.279	2.9
0.29	3.1
0.31	3.5
0.34	4
0.41	6.7

4.2 Effect of solid loading on the transition

At very low gas velocities in three-phase systems, particles are not suspended in the liquid and formed at the base of the column. As the gas velocity increased, the particles are carried by the gas bubble and some are moving downward in the entrained liquid due to gravity. Thus, based on the type of particle, formation of gas holdup in the column can be changed. The addition of non-wettable solids to air-water mixtures promotes bubble coalescence and thus reduces the gas holdup, while the addition of wettable solids suppresses bubble coalescence and increases the gas holdup (Jamialahmadi & Muller-Steinhagen, 1993). In addition, the transition gas velocity increases or decreases with increasing solid concentration.

Physical properties of particles used in this work can be seen in table 3.1 in method section.

4.2.1.1 Glass bead concentration effect

When the particle concentration is higher, the gas holdup significantly becomes lower. This was similar to the results reported by many authors (eg. Jamialahmadi & Muller-Steinhagen, 1993) who studied the effect of particle concentration on the gas holdup. García-Ochoa et al., 1997 also described that particle size influenced on the gas holdup depending on the bubble coalescence. They found that gas holdup decreases with increasing particle size. But the reason for this is unclear.

Figure 4.2.1.1 a shows the drift-flux plot as a function of gas holdup at different concentrations of 0.5mm diameter glass beads (C = 0 to14%wt.). At low particle concentrations (C<1%), the data are virtually indistinguishable from those for C = 0%. The effect of solids loading on q_{max} , the maximum gas superficial velocity corresponding to maximum gas voidage in the transition regime, can be clearly seen from these results. The corresponding results with 3mm diameter polycarbonate beads are shown in figure 4.2.1.2.

It was found that, at corresponding gas flowrates, the gas holdup was lower in the system with glass spheres as compared with the larger and less dense polycarbonate beads. A possible explanation is that the presence of small particles has a lower effect on the effective suspension viscosity compared with larger particles. Another explanation is that well suspended low density particles are not as effective in breaking up the bubble foam layer, leading to higher overall gas holdups.

At high solids loadings around 14%wt., the curves in fig.4.2.1.1a and 4.2.1.2 do not show a distinct kink as is the case for lower values of C. This is due to the high interaction between bubbles and solid particles, leading to instabilities in the flow regime, and no clear value of q_{max} can be obtained. Tzeng et al. (1993) reasoned that the development of vortices can be retarded at high solid holdups due to the disappearance of gross circulation pattern, and the interaction between solid and fluid phases become significant and results in changes in the macroscopic flow behavior.

Saxena and Chen (1994) reported that the presence of particles changes the rheology of two- and three-phase dispersions in bubble columns. Increasing solid concentration

in a liquid tend to increase the effective viscosity of the slurry. Generally, it was found that the addition of particles decreases the gas phase holdup for all types of particles. Krishna et al. (1999) added fine silica catalyst particles of 40μm to the liquid phase and found that the presence of particles promotes regime transition due to bubble coalescence.

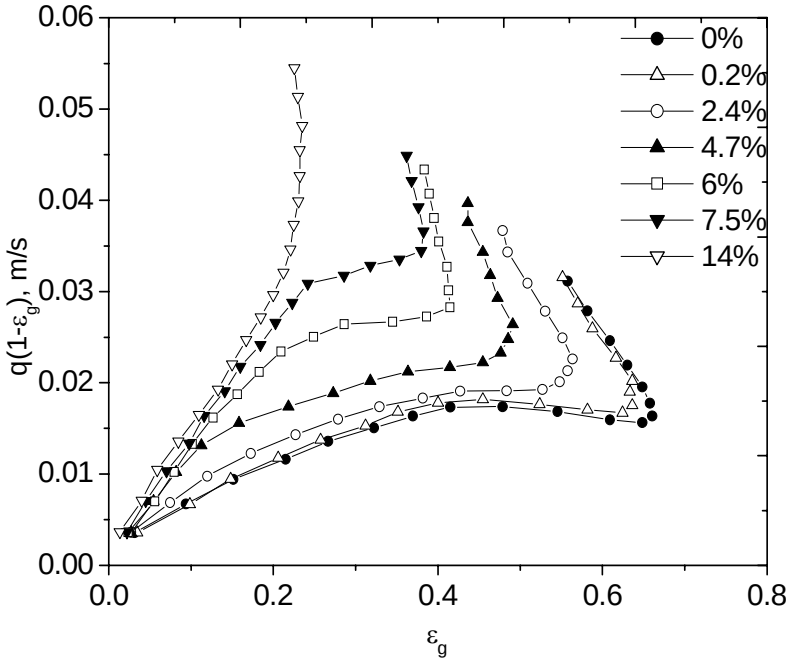

Figure 4.2.1.1 a: Characterization of q_{max} with drift flux model: effect of different concentration of glass beads 0.5mm, D = 0.15m, H /D = 3.7; plate parameters: φ = 0.2%, d_o = 0.5mm.

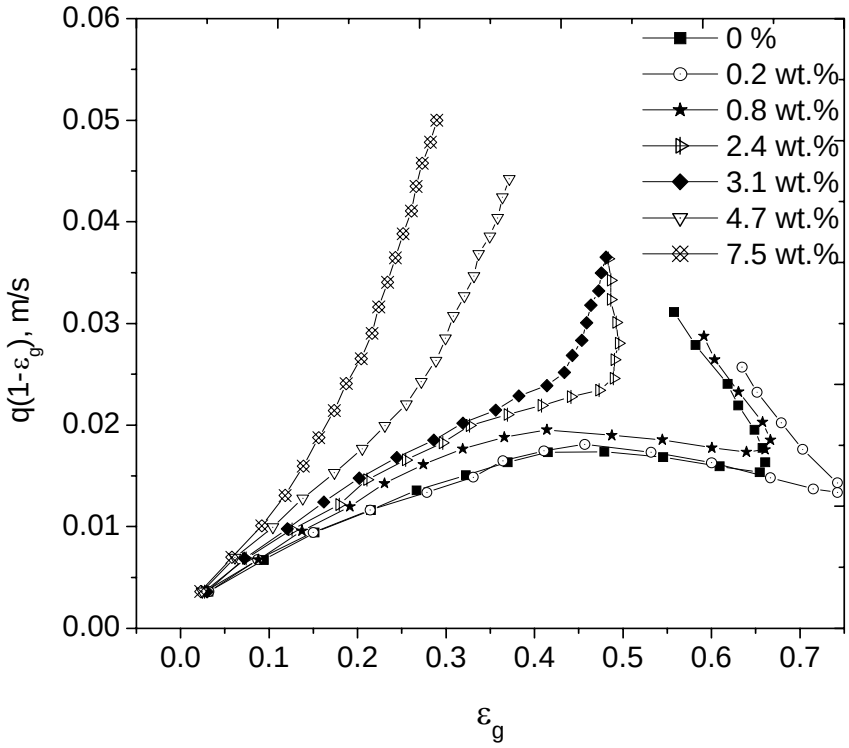

Figure 4.2.1.1 b: Characterization of q_{max} with drift flux model: effect of different concentration of glass beads 3mm, D = 0.15m, *H* /D = 3.7; plate parameters: φ = 0.2%, d_o = 0.5mm.

Figure 4.2.1.1 b illustrates that the characterization of q_{max} at various concentration of larger glass beads. The results show that even at > 4wt. % there is no transition regime obtained. It is found that large and high density particles were easily

experienced the instability of flow pattern due to the formation of wide bubble size distribution. In addition, at low gas velocity, the gas holdup curve seems to deviate from the curve of free solid indicating the heavy particles prefer to sit at the distributor and block the way of bubble formation. As a result, small bubbles are observed and reduce the gas holdup evolution.

4.2.1.2 polycarbonate concentration effect

Fig 4.2.1.2 represents the characterization of $q_{\max}$ using different concentration of 3mm polycarbonate particles. Gas holdup from experiments with smaller particles of higher density is found to be a bit lower than those with larger particles of lower density.

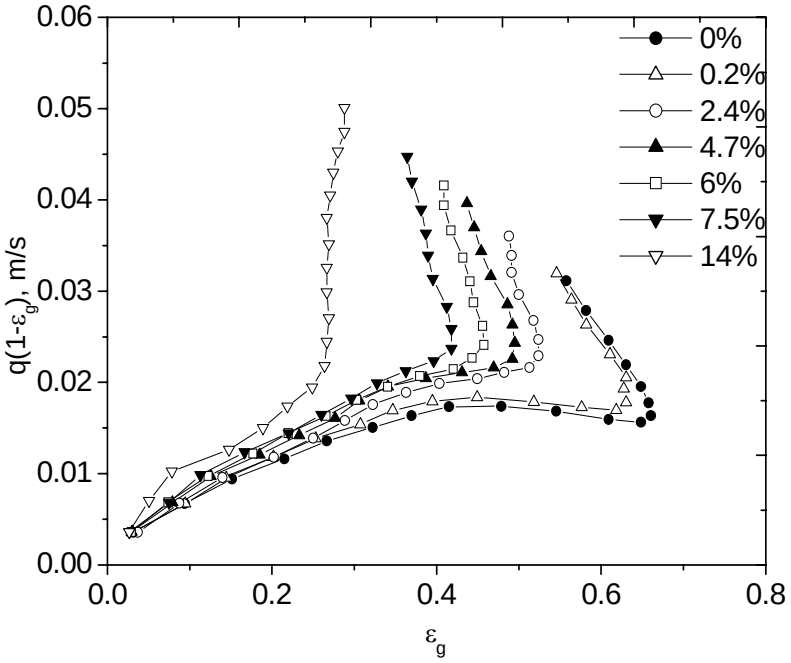

Figure 4.2.1.2: Characterization of q_{max} with drift flux model: effect of different concentration of polycarbonate particles 3mm, D = 0.15m, H /D = 3.7; plate parameters: φ = 0.2%, d_o = 0.5mm.

4.2.1.3 Different types of particles effect on transition

The effect of solids on the maximum gas superficial velocity corresponding to maximum gas voidage in the transition regime (as characterized by q_{max}) can be summarized in figure 4.2.1.3, where results for q_{max} are plotted for 3 particle types. The results show that the larger 3mm particles of glass and polycarbonate tend to promote earlier transition, as shown by the decreasing trend of q_{max} , whereas small particles (0.5mm glass spheres) tend to extend the homogeneous regime. It was also observed that in the experiments involving the larger glass spheres, the solids tended to settle towards the bottom of the bubble column. For solid concentration greater than about 3%wt. of 3mm glass spheres, complete suspension could not be achieved, and the clustering of particles above the distributor resulted in a purely heterogeneous flow regime.

In addition, particle-fluid density difference also plays an important role on the determination of transition. With high density particles, particle fluid density difference is large so that particle settling velocity would increase. Consequently, gas velocity to suspend particles would increase. Therefore, inadequacy of gas velocity to suspend the high density of large particles at high concentration leads the particle to settle near the gas distributor and makes the flow turbulent. As a result, at > 4%wt. concentration of large size and high density particle, pure heterogeneous regime is only observed.

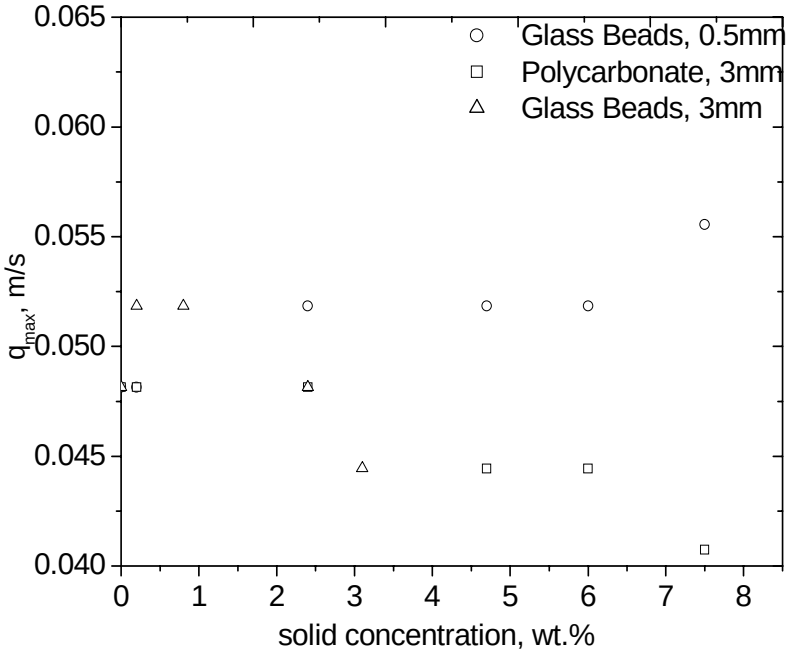

Figure 4.2.1.3: effects of three different types of particle concentration on the flow regime transition, D = 0.15m, H /D = 3.7; plate parameters: φ = 0.2%, d_o = 0.5mm.

4.3 Liquid circulation in bubble column

4.3.1.1 Characterization of flow regime in WDT and DT

Figure 4.3.1.1 represents that the drift-flux plot versus overall gas holdup in the column with draught tube (DT) and without draught tube (WDT) to determine $q_{\max}$ at maximum voidage and measure the liquid velocity at that point. Actually, the flow regime definition in DT and WDT is quite different. There are three regimes in DT namely, no air bubbles (regime I), bubbles remain stationary (regime II) and bubbles flow downwards and into the riser (regime III). There are the transitions between regimes I-II and II-III.

From the figure 4.3.1.1, it is clear that the gas holdup in regime II increases and reaches a maximum at the regime transition at a gas velocity of 0.033m/s, and decreases in regime III. In addition, the gas holdup at transition II-III is found to be 15%. For column with DT, the onset of transition towards heterogeneous flow can be identified as the point of the drift-flux curve where there is an abrupt change in gradient. The value of q corresponding to this point is $q_{\max}$, the maximum gas superficial velocity corresponding to maximum gas voidage in the transition regime.

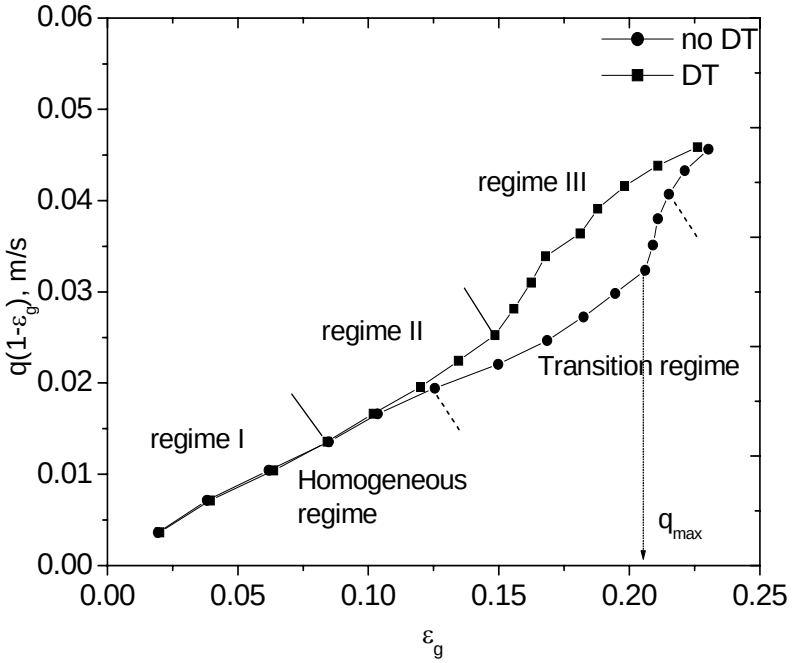

Figure 4.3.1.1: identification of critical value of superficial gas velocity for transition from overall gas holdup vs. superficial gas velocity (WDT = without draught tube, DT = with draught tube), D = 0.15m, *H*/D = 5; plate parameters: φ = 0.04%, d_o = 0.5mm.

4.3.1.2 Time averaged Liquid flow field

In Fig. 4.3.1.2, the profiles of the time averaged flow field of the liquid were determined by averaging the information of 30 dual frames PIV vector fields per profile with a height of 0.03-0.11m at the gas velocity of q = 0.04 m/s.

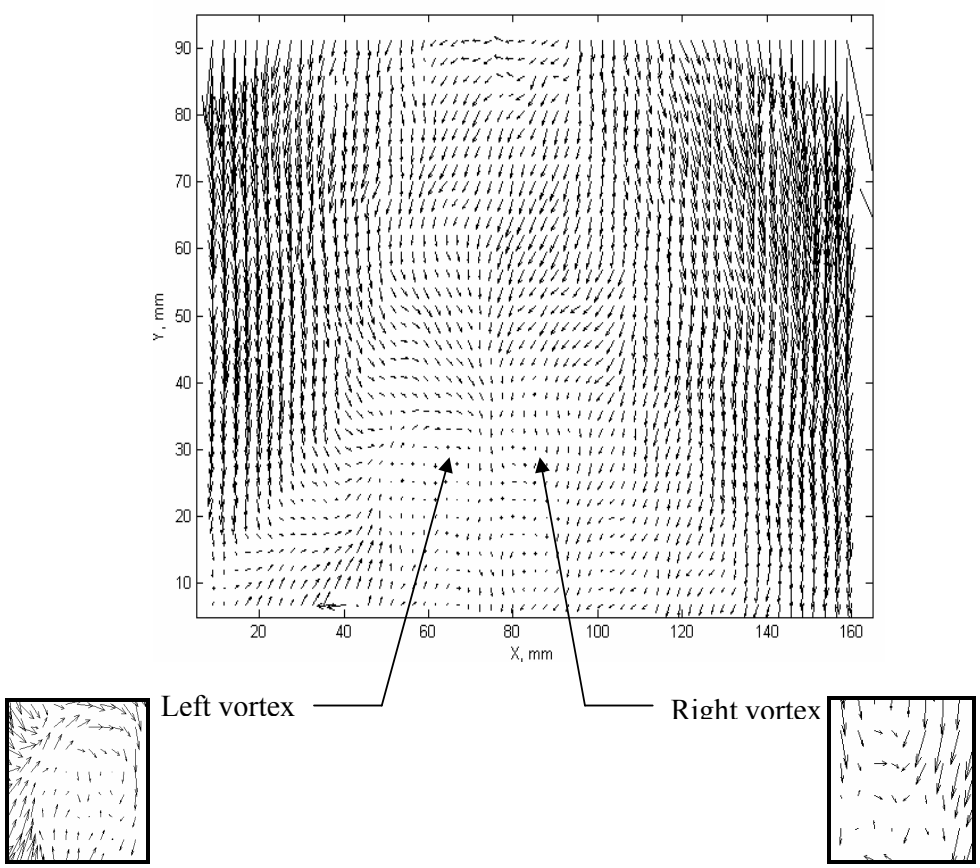

Figure 4.3.1.2: Vector plot of Time averaged 2-D liquid flow field at transition gas velocity (q = 0.04 m/s) in the bottom of column with draught tube at wall region, D=0.15m, n=49, H=0.55m.

It is observed that the existence of a pair of liquid vortex in time averaged flow field is caused by the liquid circulation structure which consists of a bubbly upward flow in the column core region and bubble-free liquid downward flow region near the side wall (Fig. 4.3.1.2). It is more likely to be influenced near the gas distributor region. At low gas velocities, gross liquid circulation is not observed. Deckwer, 1992 reported that a radial cross-exchange of fluid elements leads to axial circulation pattern and gives rise to high radial intermixing.

In the heterogeneous regime, liquid downflow was very pronounced. At gas velocities intermediate between those causing homogeneous and heterogeneous regimes, the trend of bubble streams appears to oscillate in the column core and to show a tendency towards recirculation. Simultaneously, vortices appear near the sidewall caused by the momentum transfer to central region from wall region. These vortices have been termed descending vortices (Tzeng et al., 1993). This transitional flow pattern is similar to that suggested by Olmos et al. (2003) using wavelet transforms.

4.3.1.3 Interpretation on wall region flow

The downward liquid flow region near the sidewall represents the descending flow region (Tzeng et al., 1993). There appears to be no bubbles occupying this region at very low gas velocities. As the gas velocities increase, small bubbles were observed in the descending liquid as evidenced by small scale liquid recirculation.

In the case of the fluid flow field without DT, a vortical flow region is observed close to the descending flow region (Fig.4.3.1.2). Vortices seem to be formed at the

confluence of descending liquid flow and the upward bubble plume region. The sizes of vortices increased in size and instability with increasing gas velocities. The development of vortical structure near the wall is disappeared with the presence of DT and pure descending region is only observed at wall region (Fig.4.4).

A third region may be discerned in Fig.4.3.1.2 which is the central descending region located between the two vortical flow regions. This central region is characterized by complex flow associated with bubble wakes or liquid slip flow between bubble streams in the core region. The size of this region depends on the geometry of the column. In this region, the liquid velocity is lower than that in the sidewall region.

In the middle section of bubble column (y=0.2-0.3m), downward motion is only seen. No influence of gas distributor effect is found.

4.4 Liquid circulation in draught tube column

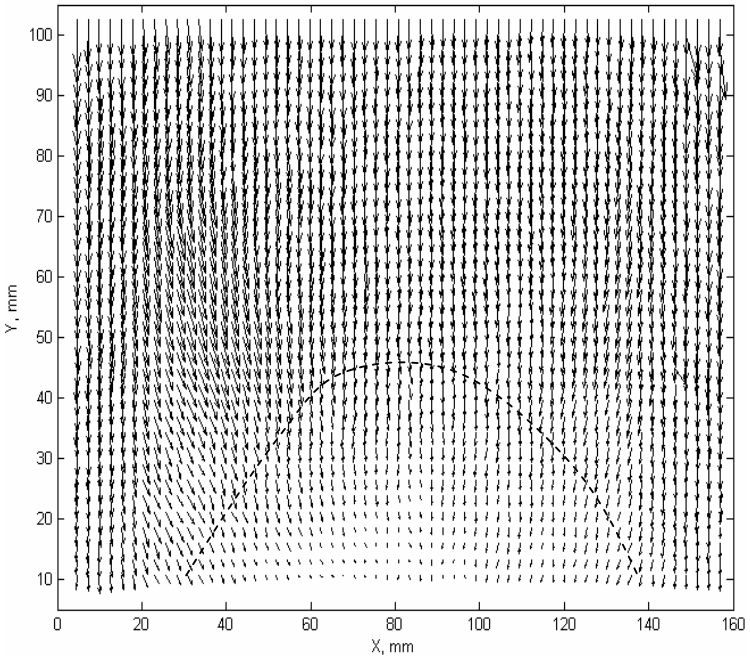

Figure 4.4: Vector plot of Time averaged 2-D liquid flow field at transition gas velocity in the bottom of bubble column with draught tube, D=0.15m, n=49, *H*=0.55m.

Fig. 4.4 shows the time averaged flow field at q = 0.04 m/s in the column with DT. The results show a predominant downflow near the wall region, showing the effectiveness of the DT in facilitating liquid circulation. The area enclosed by the dashed line is the region where the liquid changes direction prior to entering the riser. A similar flow pattern was observed for all values of gas flowrate. No wall-region vortex was observed in the case of columns with DT.

There may be some vortex at the downright of draught tube bottom where the liquid from annulus migrating to the riser and meet with upflowing liquid carried by bubble plume in the riser. In the middle section, same phenomena are observed. Velocity distribution is quite uniform.

4.5 Reynolds stress identification

The Reynolds stress is described by the mean and fluctuating velocities of the liquid circulation induced by the bubble. In a turbulent flow, the fluctuating velocity field is defined by $u(x,t) = U(x,t) - \langle U(x,t) \rangle$. The (one point, one-time) covariance of the velocity $\langle u_i(x,t) u_j(x,t) \rangle$ is called Reynolds stress, and is written as $\langle u_i u_j \rangle$ where i and j shows the directions. The Reynolds stresses can be calculated by the instantaneous velocity of various frames. The vertical normal stress is found to be nearly twice the horizontal normal stress. This is in agreement with the results in Olmos et al. (2003).The formation of two circulation cell structures near the wall is also observed in Reynolds stress patterns.

Fig.4.5a shows the typical Reynolds stresses profiles at various radial positions in a bubble column with no DT. The vertical normal stress profile is flat in the middle with two distinct maxima close to each sidewall. The horizontal normal stresses on the other hand, display a flat maximum in the centre and minima at the walls. Our earlier observation of vortices migrating towards the core region could explain the result that vertical normal stresses are higher at the walls. The Reynolds shear stresses are generally lower than the normal stresses. Similar profiles for Reynolds stresses have been reported by Olmos et al. (2003) in a two-dimensional bubble column. Mudde et al. (1997a) reported that the shear stress had its greatest absolute value in the region where the axial velocity gradient was highest and had a value of zero where the averaged axial velocity was maximum according to the Boussinesq type of correlation between the averaged axial velocity and the shear stress.

In Fig.4.5b, the typical Reynolds stresses profiles are shown for a bubble column with DT since no vortices are formed, normal stresses are lower as compared with fig.4.5a, and the shear stresses are virtually zero. The DT allows a regular circulation pattern of liquid upwards in the central DT and downwards through the annulus and this clearly serves to stabilize the overall column hydrodynamics. The maximum magnitude of normal stresses can be seen in table 4.5. The results show that the fluctuation was higher in no DT column than in DT column.

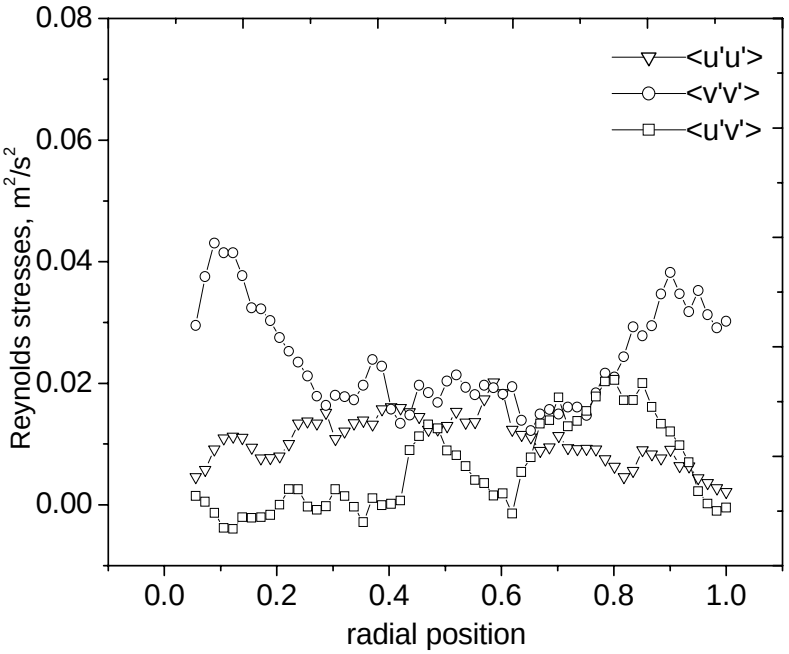

(a) WDT

Figure 4.5: Profile of Reynolds stresses in the bottom of the bubble column (a) WDT (b) DT, D=0.15m, n=49, *H*=0.55m.

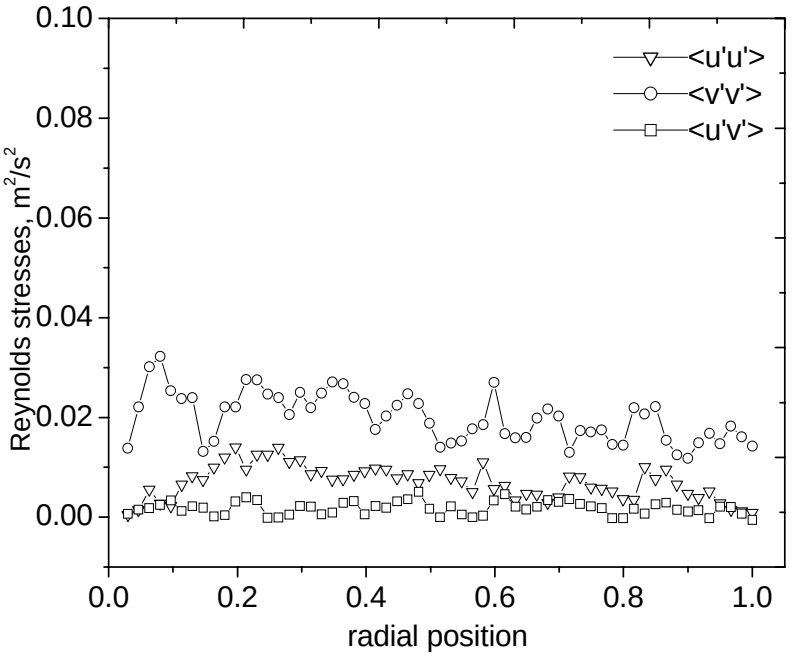

(b) DT

Figure 4.5: Profile of Reynolds stresses in the bottom of the bubble column (a) WDT (b) DT, D=0.15m, n=49, *H*=0.55m.

Table 4.5: Maximum magnitude of the Normal Stresses in the column with and without draught tube

Column	Section	$\langle u'u' \rangle$ (cm^2/s^2)	$\langle v'v' \rangle$ (cm^2/s^2)
with DT	bottom	200	900
	Middle	350	620
without DT	bottom	670	1100
	Middle	460	850

4.5.1.1 Influence of gas velocity

Fig.4.5.1.1 a and b show the effect of gas velocity on the shear stress pattern in WDT and DT. Different gas velocities of 0.022, 0.029, 0.04, and 0.06m/s were applied. The shear stresses are nearly zero at all gas velocity in this wall region measurement except at very high gas velocity. It shows that there is no or little net transport from axial momentum in the tangential direction. Thus, the fluctuation is less at the wall region in the column with or without draught tube.

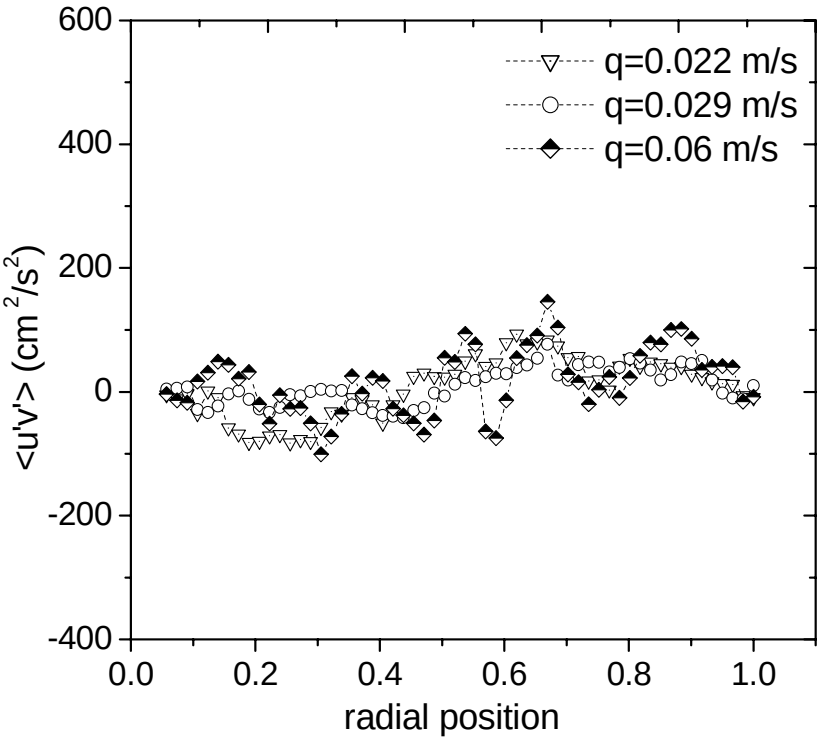

(a) WDT

Figure 4.5.1.1: Effect of gas velocity on the Reynolds stresses at the bottom section of the column (a) WDT at q=0.022, 0.029, 0.06 m/s (at ε_g = 12%, 17%, 23%).

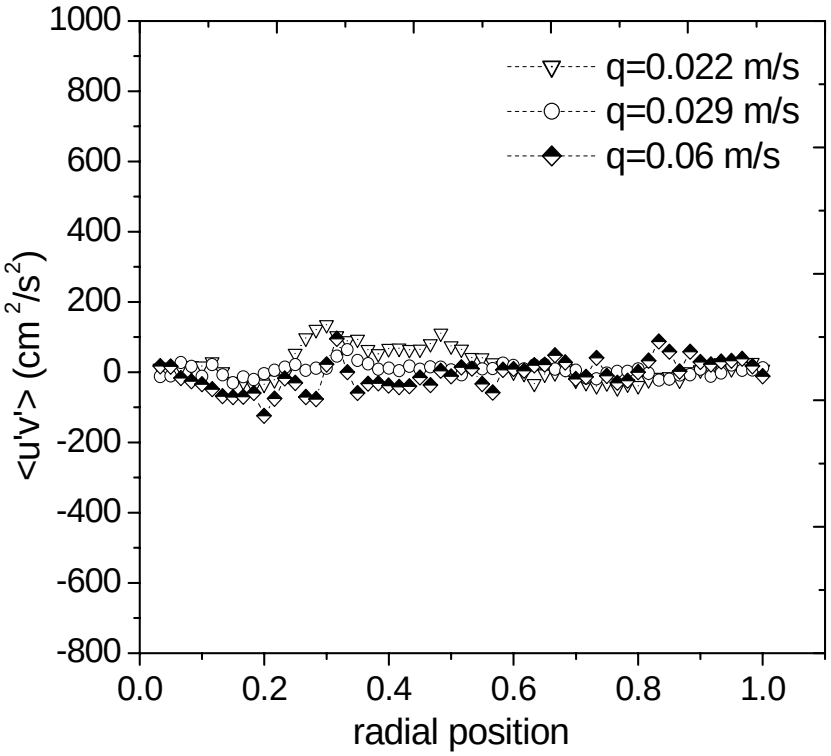

(b) DT

Figure 4.5.1.1: Effect of gas velocity on the Reynolds stresses at the bottom section of the column (b) DT at q =0.022, 0.029, 0.06 m/s (at ε_g = 12%, 15%, 23%).

4.5.1.2 Centerline velocity

Fig.4.5.1.2 a, depicts the averaged centerline velocity, <v> vs different axial location at various superficial gas velocities in DT column. Centerline velocity in DT increases with increasing gas velocity. Above y/h=0.7, the velocity becomes constant with axial direction. Thus, uniform distribution can be seen in the middle section showing no effect of gas distributor.

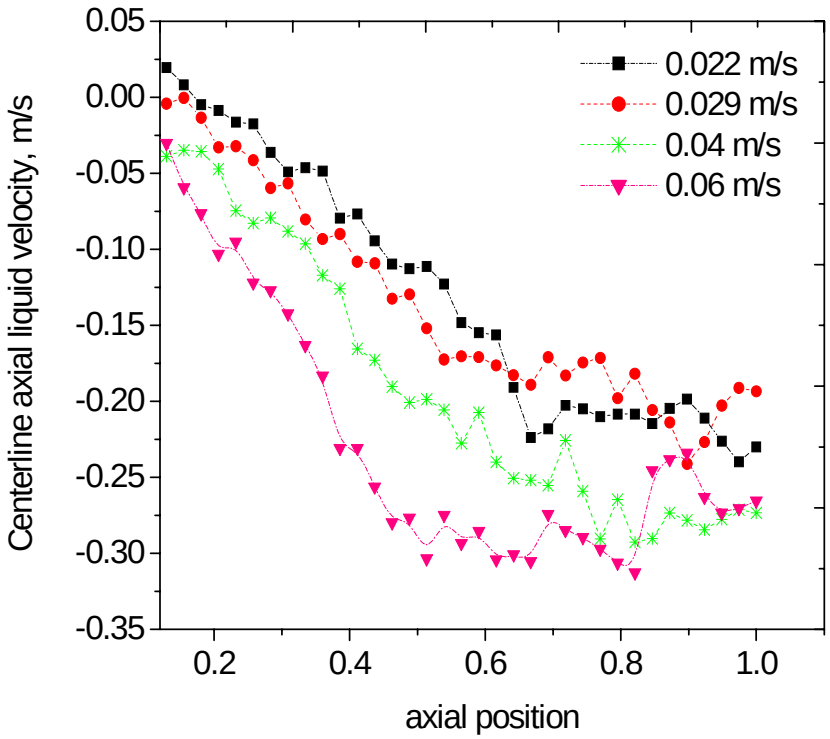

(a) DT

Figure 4.5.1.2: Measured centerline axial liquid velocities 0.03 m above the plate sparger in (a) DT for different superficial gas velocities.

Fig.4.5.1.2 b, depicts the averaged centerline velocity, <v> vs. different axial location at various superficial gas velocities in WDT column. Centerline flow structure in WDT, due to the disturbance of vortical structure, is not as regular as in DT. Depending on the movement of bubbly flow structure, the flow phenomena of axial centerline velocity is obtained especially in the small column like this work. The region for centerline is rather small.

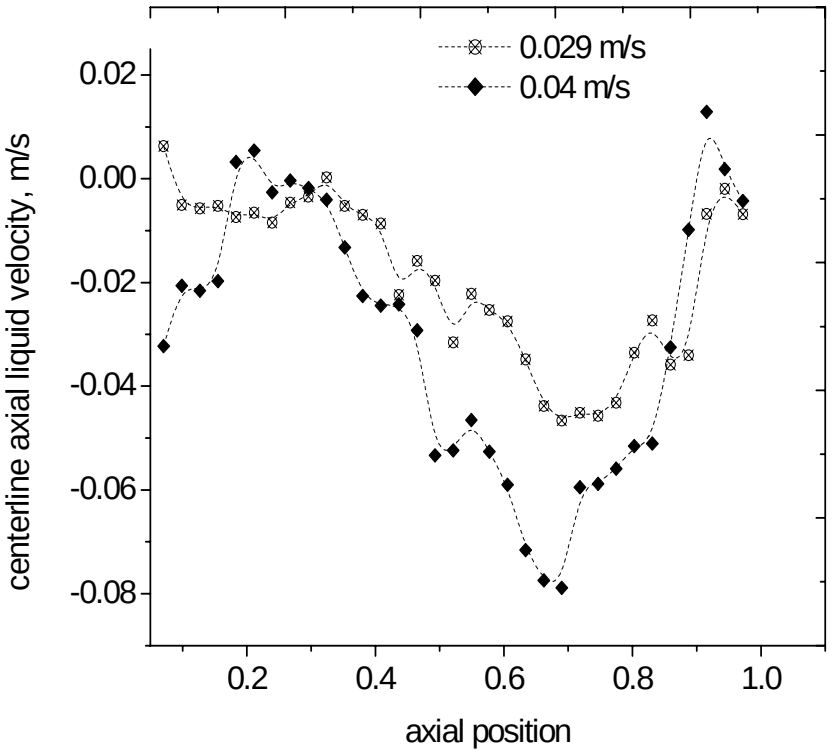

(b) WDT

Figure 4.5.1.2: Measured centerline axial liquid velocities 0.03 m above the plate sparger in (b) WDT for different superficial gas velocities.

4.5.1.3 Axial velocity in the middle section

Figure 4.5.1.3 indicate that axial liquid velocity profile at the middle section in DT column at 0.055 m/s. Axial velocities at sidewalls in the middle section are higher than those in the bottom. This figure represents that the flow structure is not changing with axial position.

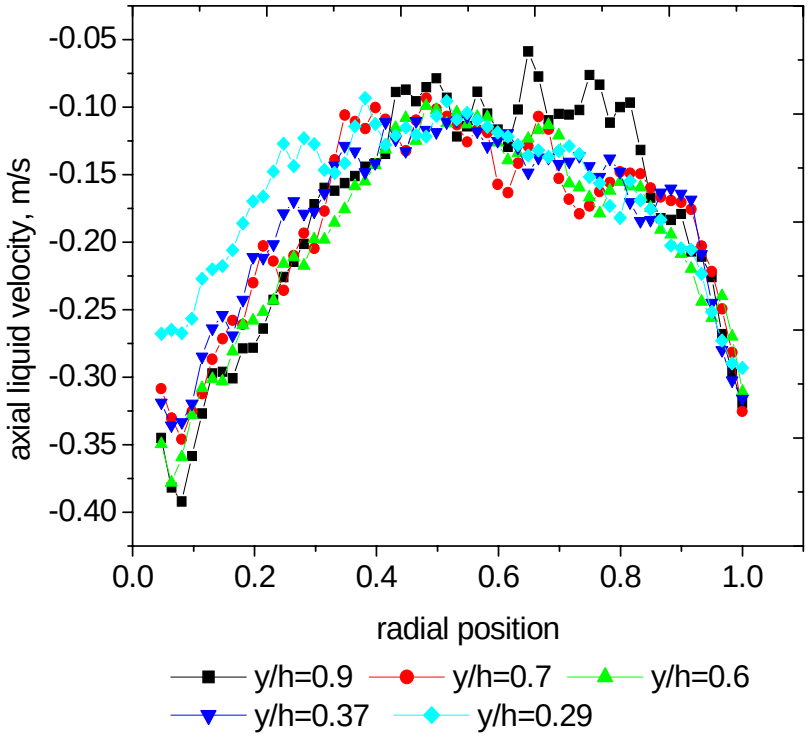

Figure 4.5.1.3: axial liquid velocity profile at different y of the middle section in DT column at q_{max} , D=0.15m, n=49, *H*=0.55m.

4.6 Partial aeration in bubble column

Previously (Borchers et al., 1999, Becker et al., 1999 and refs: there in), the gas was introduced from the column center and reported that the symmetrical flow field with liquid upflow in the column center and liquid downflow along the side walls. But Becker et al., 1994 introduced the decentralized gas inlet and found that only large liquid vortex on the right hand side as they applied left aeration. The bubble plume was stable and directed to the left wall. Here, the work on centralized and decentralized gas inlet will be considered and the spatial resolution of PIV based on the peak formation of different number of orifices from time averaged surface plot will be discussed. In addition, Reynolds stresses caused by disturbance of bubble formation from different orifices will show the liquid flow field related to the influence of bubble formation.

The gas in this section will be dispersed at 10.4m/s. Because the orifice size of > 1mm will greatly influence on the bubble size based on the gas velocity. Increasing bubble frequency at high gas velocity promotes the bubble coalescence rate which leads to large bubble formation. And the reflection from the large bubbles has a major disturbance to the resolution of PIV even though the measurement was focused on liquid phase in the present study. In addition, the tracer particles may be hidden by blockage of bubbles from laser light as well as the inadequacy of tracer particles at the bottom and middle sections since these are carried by the bubble plume to the top at high gas velocity and consequently decrease the resolution of PIV.

4.6.1.1 Influence of aeration

4.6.1.1 Single aeration effect

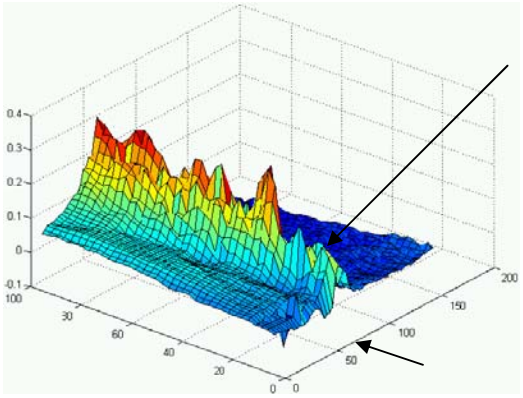

(a)

Figure 4.6.1.1 (a) Time-averaged surface plot of liquid flow pattern using single orifice.

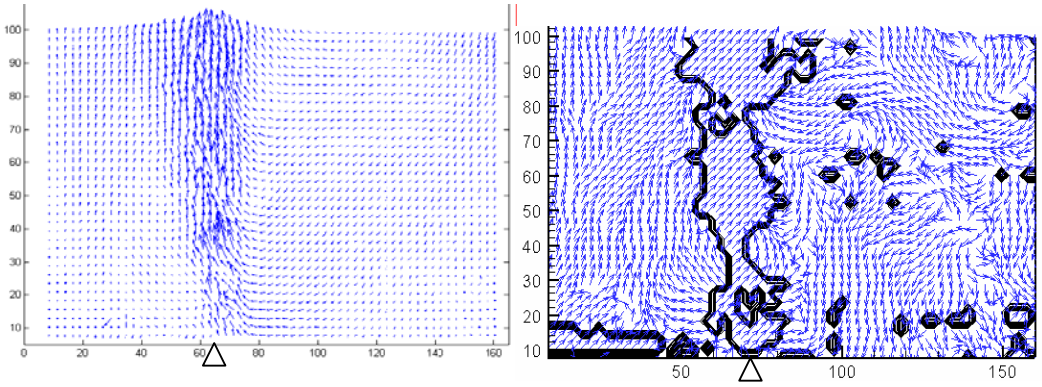

(b) (c)

Figure 4.6.1.1 Comparison between time averaged and instantaneous two dimensional flow field using single orifice (b) time averaged flow pattern (c) instantaneous flow field.

Figure 4.6.1.1 (a) depicts the time averaged liquid flow pattern from 30 frames. Liquid flow around single bubble passage closer to the left wall can be seen. This is because the gas is dispersed from the left side of the column. The color shown in surface plot shows the intensity of the turbulence. Along the bubble stream, the liquid flow structure is more chaotic caused by the bubble. Right side of the column is stable and moving downward. This is due to the fact that the liquid carried by the bubble falls back when the bubble reaches to the surface. The wider bubble stream can be observed from fig.4.6.1.1 (b) when the bubble is away from distributor and it shows that the bubble coalescence at a higher distance from the bottom and move in a swinging motion after it detached from the orifice. No vortex can be observed at bottom part of the column with single bubble stream. fig.4.6.1.1 (c) is the instantaneous vector field with contour showing similar flow structure of time averaged flow field. The liquid flow at the passage of bubble shows stagnant in this figure. Some small contour at right side of bubble stream may be caused by the small bubbles which are broken by the large bubble plume or insufficient tracer particles due to the blockage of bubble stream.

For centralized gas inlet, Borchers et al., 1999 found that H/D >1.5 at 0.4125 mm/s gas velocity, two staggered rows of vortices moving downward in a period way. However, the vortex forming seems depend on the operating conditions such as the column dimension, superficial gas velocity and sparger design. If the column is small there is needed to be considered the wall effect and placement of aeration to determine the number of cell forming in the column.

In Figure 4.6.1.1, since the distance from the bubble to each of the two sidewalls is different, the liquid momentum transferred from the rising bubble is dissipated at uneven rate. This uneven dissipation rate of momentum yields an asymmetric liquid velocity profile to the bubble center and results in a higher pressure at the side closer to the left-wall where close to bubble distributor. This lateral pressure difference causes the downward circulation at near the right-wall.

In the middle section, liquid vortex was observed at the right corner of the column. This is obtained by the liquid circulation when bubbles reach to the surface and entrained liquid move downward motion and meet with the up-flowing liquid together with the bubble. Together with the top section, there are three small scale vortex can be observed in the whole column. This finding is consistent with Becker et al., 1994. Due to the uneven gas distribution, gross circulation is developed in the whole column.

4.6.1.2 Double aeration effect

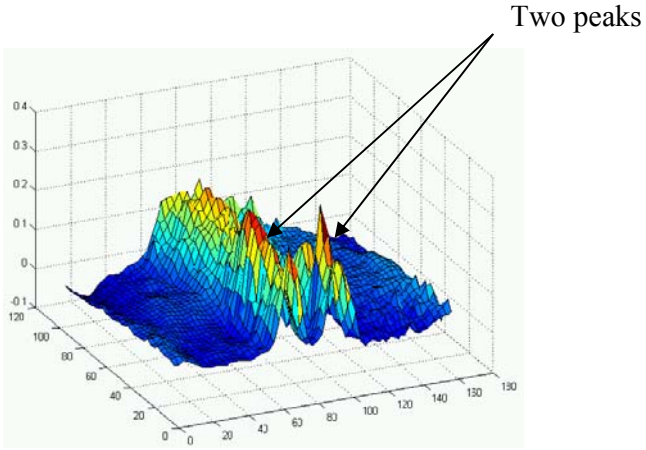

(a)

Figure 4.6.1.2 (a) Time-averaged surface plot of liquid flow pattern using double orifice.

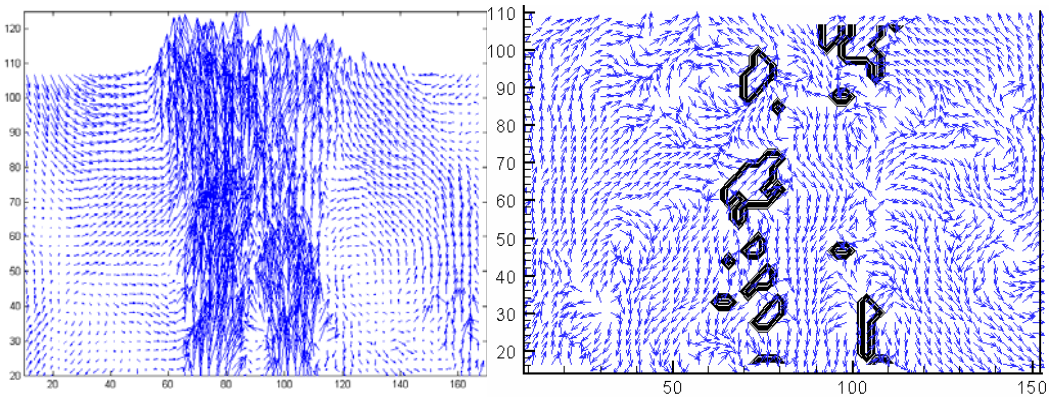

(b) (c)

Figure 4.6.1.2 Comparison between time averaged and instantaneous two dimensional flow field using double orifice (b) time averaged flow pattern (c) instantaneous flow field.

Figure 4.6.1.2 shows the effect of double orifice in the bubble column. After averaging, the results still maintained the two significant bubble streams. The bubble plume is not stable and beyond the critical height of the liquid, it behaves as single bubble stream. The distance from the bottom to the coalescence region may be related to the orifice spacing between two distributors. In addition, the size of the bubble which depends on the orifice size may also be responsible. Due to the centralized aeration of two distributors, the vortex forming is occurred in both sides of bubble flow.

Figure 4.6.1.2 (b & c) involves the comparison between time averaged and instantaneous flow field. Two large scale vortexes are forming each side of the two bubble streams in both flow fields. In Figure 4.6.1.2 (b), some downflow liquid can be observed under the bubble contour. This may be caused by the bubble wake and we can see clearly the stagnant flow in the shape of contour as it is the place of bubble.

4.6.1.3 Tetra aeration effect

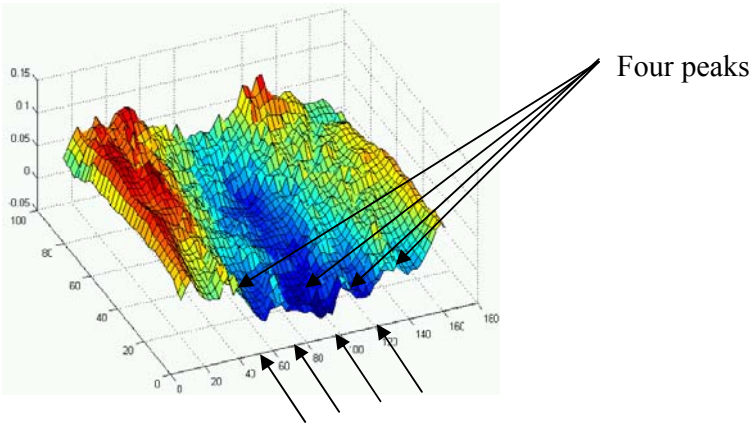

Figure 4.6.1.3 (a) Time-averaged surface plot of liquid flow pattern using tetra orifice

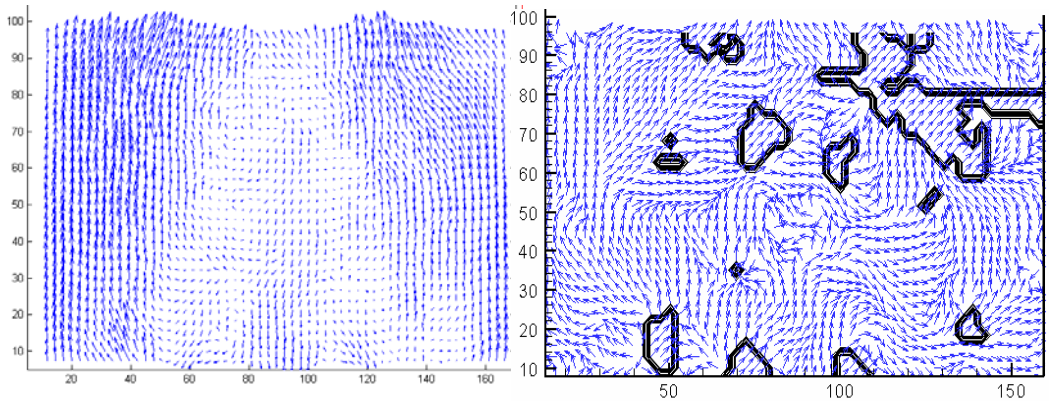

Figure 4.6.1.3: Comparison between time averaged and instantaneous two dimensional flow field using double orifice (b) time averaged flow pattern (c) instantaneous flow field.

Figure 4.6.1.3 represents that time averaged liquid flow pattern in the bubble column with four spargers. The surface plot shows four peaks from four orifices. Certain distances from the bottom, four bubble peaks combine and form one passage. The liquid downflow is observed between bubble streams. That might be caused by the bubble which coalescence and entrained the liquid.

In the middle section, two small scale vortex form at closer part of top region and near the wall. Both are caused by the wall effect and thus left vortex is in the anticlockwise from the left wall and right vortex is in the clockwise direction from the right wall. From this time averaged flow patterns, it is observed that time averaged flow structure of transient flow is the same as the instantaneous flow structure. That shows the measuring time in this case is sufficient to produce long time averaged flow pattern.

In the top section of all conditions, two vortex form at both left and right sides of the column. The number of small scale vortices may increase with number of aeration.

4.6.1.4 Effect of bubble coalescence in the column

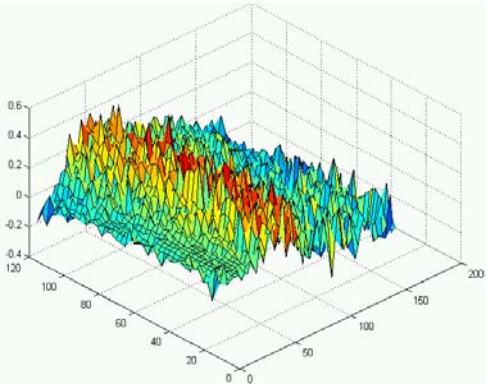

(a)

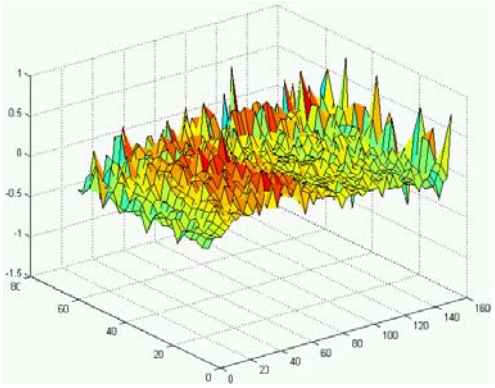

(b)

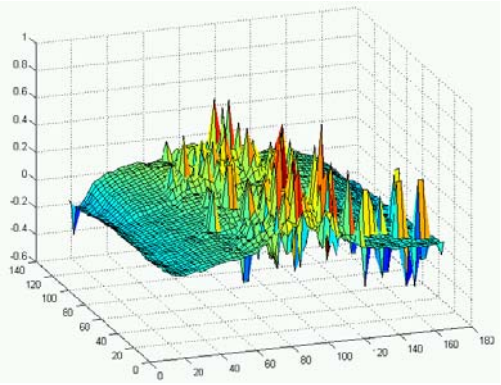

(c)

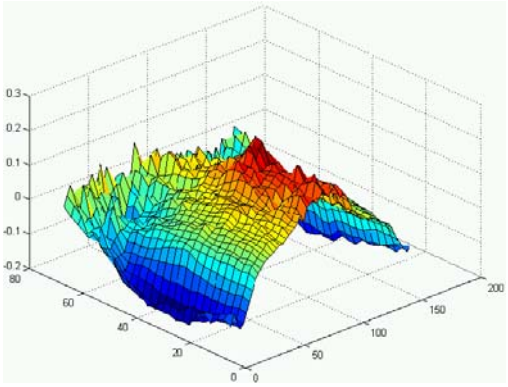

(d)

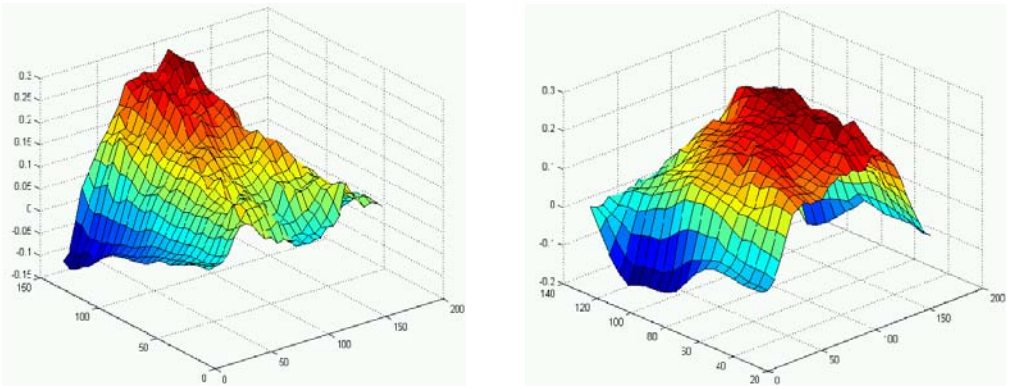

(e) (f)

Figure 4.6.1.4 Time averaged surface plot at middle and top section of the column, single aeration (a) middle (b) top, double aeration (c) middle (d) top, tetra aeration (e) middle (f) top.

Time averaged surface plot of middle and top sections of the column is different with number of orifices used (Fig. 4.6.1.4). For single orifice, the bubble plume is flowing straight until surface. But in Figure 4.6.1.4 (b), due to the coalescence of the two bubble stream, chaotic forming is observed in the middle of the column. Bubble coalescences occur because neighboring bubbles are close to each others. It is significantly dependent on the size of orifice and orifice spacing between two successive orifices.

In the top part, there is no significant bubble plume route found and the same as the middle and top section of column with tetra aeration (Figure 4.6.1.4 (e & f)). Here, liquid velocity decrease with increasing gas distributors, i.e. when the bubbles are taken the place in the column and the liquid does not have the space and lowest liquid velocity is found in the column with four orifice gas inlet.

4.7 Reynolds stresses on flow structures

The measurement of Reynolds stresses allows a first characterization of liquid macrostructures and of the related bubble influence. As already explained that the instantaneous flow pattern is nearly the same as time averaged flow pattern, Chen et al., 1994 argued that the instantaneous macroscopic phenomena were lost when the flow information was averaged. To provide complete understanding on the instantaneous behavior of bubble columns, more analysis on smaller scales or microscopic phenomena is required. This can represent with the liquid phase in the form of fluctuating velocities, turbulence intensities, and Reynolds stress terms. For the case of high void fraction as multiple aeration system, if the time is not long enough the averaged flow pattern will not be the same as instantaneous flow field.

4.7.1.1 Single aeration effect

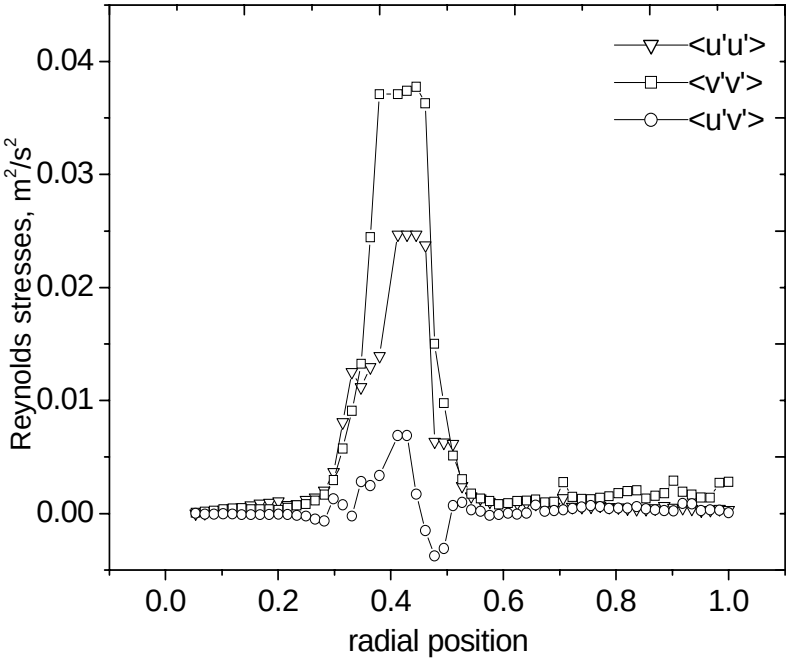

Figure 4.7.1.1 Profiles of the Reynolds stresses component for the bottom section of the column at using single aeration.

The strength of the Reynolds stresses component for the bottom section of the column can be seen in figure 4.7.1.1. Interestingly, the profiles of $< u'u' >$ and $< v'v' >$ are high in the center in this partial aeration system. When the single orifice is applied from the left side of the column, normal stresses are zero at the sides of the wall, i.e. the liquid carried by the bubble stream seems to be very large compared to the liquid away from the bubble. The velocity caused by horizontal displacement is also high in

the place of bubble. That can be explained that the bubble is not going straight and swinging motion from side to side. Thus, the normal stress due to horizontal direction can be seen large in the place of bubble stream. This phenomenon is therefore different from uniform distribution system with small orifices. The macro-scale structure is more likely to influence in that system and single peak is preferred to influence in the single aeration system. Therefore, normal stress profiles behave as the shape of bubble motion.

4.7.1.2 double aeration effect

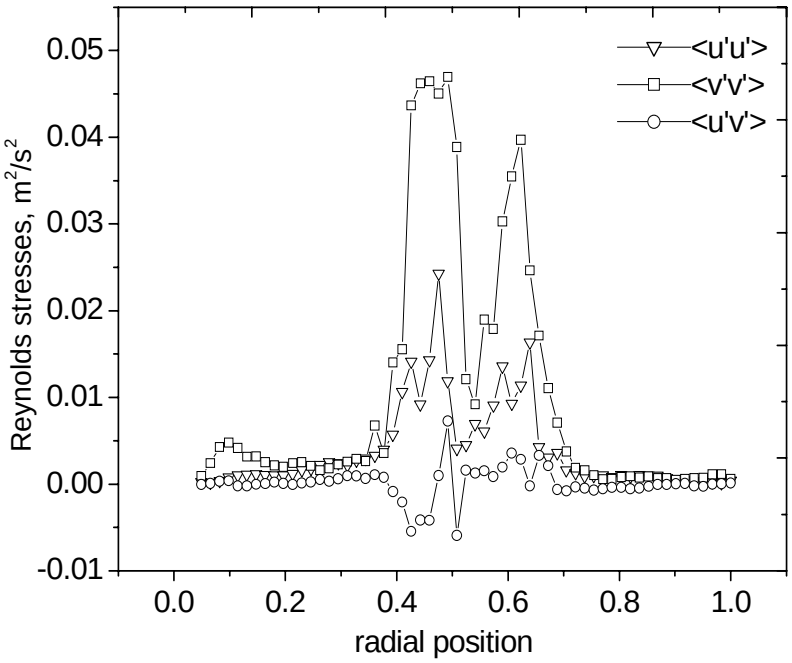

Figure 4.7.1.2 Profiles of the Reynolds stresses component for the bottom section of the column at using double aeration.

The similar observation can be seen in Figure 4.7.1.2. The difference is that this figure is the result of double aeration so two peaks formation is seen. But this time aeration is symmetrical from left to right of the column and consequently, stresses are very large in the center. Horizontal normal stresses always have similar phenomena to the vertical normal stress profile but lower in these partial distribution systems. It seems that while the bubble rise wavelike manner, small scale vortices are forming along the curve of bubble plume. That reflects the normal stresses peaks along the bubble streams. Obviously, near the wall $< u'u' >$ and $< v'v' >$ drop to zero since both u and v become zero at the wall. And shear stresses are almost zero and lower than normal stresses. But some fluctuation can be obtained in the central region somehow $< u'v' >$ can be positive and negative.

4.7.1.3 Tetra aeration effect

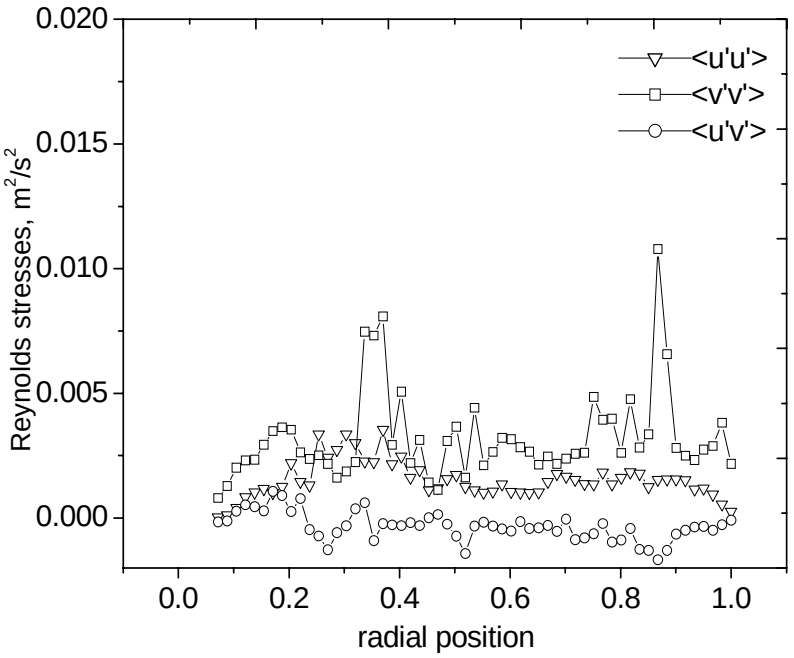

Figure 4.7.1.3 Profiles of the Reynolds stresses component for the bottom section of the column at using tetra aeration.

Figure 4.7.1.3 shows that the profile of the Reynolds stresses component for the bottom section using tetra aeration. The measured Reynolds stress values are rather low. These data may not be reliable because of limitations of the PIV measurements in a region of very high gas holdup close to the multiple orifices. Thus, for the case of multiple orifices, the measurement section is recommended to every 5 or 10 mm to obtain the changes of the bubble path because PIV can capture the area only on the

laser sheet thickness. Here, lower orifice spacing and relatively small orifice size can create the Reynolds stress profiles peak in the center.

4.7.1.4 Different aeration on Reynolds stresses in the middle section

Figure 4.7.1.4 below describes that Reynolds stresses of different aeration occurred in the middle section of the column. Larger stresses are obtained in the middle compared to these in the bottom section. Especially, the single aeration is likely to have higher Reynolds stresses and oscillate most in the laser sheet taken in the place of bubble.

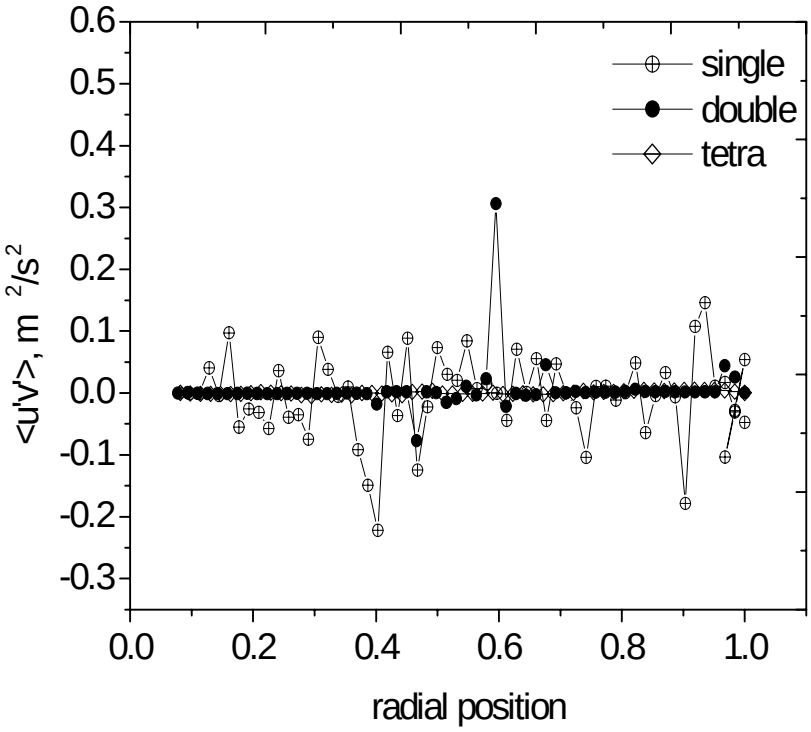

Figure 4.7.1.4 Profiles of the Reynolds stresses component for the middle section of the column at q = 10.4 m/s using different aeration.

4.7.1.5 Wall region measurement

The flow structure in this region can be either upward or downward depending on the gas velocity.

At wall region of single aeration system, descending flow near left wall and vortex forming near right wall. That vortex seems to be moving from bottom to top so that it can be seen in every test section.

At wall region of double aeration system, upward motion in the column center and downward motion is observed at sidewalls creating two vortices beside the two bubble streams.

At wall region of tetra aeration system, only upward motion is found at the bottom section and two small scale vortices is observed in the middle.

It seems that liquid circulate from bottom as well as top of the column. This is more likely to occur with low aspect ratio. In contrast to uniform aeration system, in which descending flow is mainly occurred at wall region except at distributor region.

CHAPTER 5 CONCLUSIONS AND RECOMMENDATION

5.1 Conclusions

5.1.1 Conclusions from influencing factors on transition

The study examined the effect of solid particles and liquid viscosity on the transition regime in a fully aerated bubble column. Increasing solid particles and liquid viscosity decreased the overall gas holdup. However, our results suggest that solid particles either promote or inhibit the transition gas velocity according to the size and density of particle. Earlier transition was observed with large and high density particles.

Experimental data obtained in aqueous solutions of glucose demonstrated significant effect of viscosity on the transition gas velocity. Increased viscosity of liquid phase promoted the transition regime and enhanced the instability of homogeneous regime at μ_L > 4mPa s. Moreover, transition gas velocity was found to decrease with increasing aspect ratio in glucose aqueous solution. This result was the same observations occurred in air-water two phase systems and is expected to maintain the stability of transition by the addition of surface tension reducing agents.

5.1.2 Conclusions from uniform aeration

In this work, the time-averaged liquid mean velocity profiles have been measured using PIV in a bubble column with the presence and absence of draught tube up to gas holdup values of 23%. The liquid circulation structure at wall region has been reported in the transition regime, but this structure is eliminated with the addition of draught tube. Furthermore, this liquid vortex structure has been evaluated by Reynolds stresses patterns.

The fluctuation velocity in the bottom and middle section of the column in the wall region was attained by introducing the sufficient tracer particles. The Reynolds stresses in WDT was larger than those in DT reflecting the influence of vortical structure. Flat profile in the middle and peak both sidewalls are formed for vertical normal stress. In addition, Normal stresses are always higher than shear stresses showing anisotropic turbulence.

This study fills up the needs for the understanding of the flow regime transition in the bubble columns and airlift reactors (Vial et al., 2001).

5.1.3 Conclusions from partial aeration

Liquid flow structure in the bubble column was experimentally investigated using single to tetra orifices. The strong influence of the sparger on the resolution of PIV has been highlighted by the evolution of time averaged surface plot and Reynolds stresses. Reynolds stress profile of partial aeration was found to be opposite to those

obtained with uniform aeration. Because reverse phenomena for Reynolds stress profiles, peak in the middle and flat profile at both sidewalls was observed for vertical normal stress. Normal stresses are always higher than Reynolds stresses.

The following were summarized from the contribution of this research:

1. Placement of gas distributor is an important parameter for liquid flow structure. It was found that the placement of vortex depended on the flow pattern of bubble stream.
2. Orifice size may also influenced the formation of bubble because the larger the orifice, the higher the bubble frequency. Microscopic flow structure containing bubble coalescence and breakup was improved by the bubble frequency. The number of small scale vortices may increase with number of aeration due to increasing number of bubble frequency. Alternately, these coalescence rates affect the peak formation of surface plot in liquid flow structure.
3. Another important parameter is the column dimension, i.e. lower aspect ratio was supposed to increase the liquid circulation in the column and that reflected the number of vortex forming.
4. Gas velocity as well as the system pressure introducing to the gas chamber could not leave out to study the liquid flow structure. Higher gas velocity provides the larger vortex size. To capture the vortex forming, long time measurement was required.

5.2 Recommendations for future study

1. Hydrodynamics of a bubble column containing binary mixture of different size and density particles will be interesting.
2. Proposing mathematical model for gas velocity transition under the effect of viscosity and solid concentration.
3. Study the flow pattern changes and fluctuating velocity by varying the inlet jet height to the column.
4. Gas density effect on the fluctuating velocity and Reynolds stress that will lead to larger bubble size and higher liquid velocity. Consequently, the vortex forming will also be changed.
5. Changes of entrance length to coalescence two bubble streams by varying the orifice spacing. PIV spatial resolution will also be changed in this system. To provide complete understanding on the instantaneous behavior of bubble columns between coalescencing and non-coalescencing medium, more analysis on smaller scales or microscopic phenomena is required.

REFERENCES

Becker, S., Sokolichin, A. and Eigenberger, G. (1994). Gas-Liquid flow in bubble columns and loop reactors: Part II. Comparison of detailed experiments and flow simulations. *Chem. Eng. Sci*., 49, 5747-5762.

Becker, S., De Bie, H. and Sweeney, J., (1999). Dynamic flow behaviour in bubble columns. *Chem. Eng. Sci*., 54, 4929-4935.

Borchers, O., Busch, C., Sokolichin, A. and Eigenberger, G. (1999). Applicability of the standard k-ε turbulence model of the dynamic simulation of bubble columns. Part II: Comparison of detailed experiments and flow simulations, *Chem. Eng. Sci*., 54, 5927-5935.

Br¨ucker, C. (1996). 3-D Scanning-Particle-Image-Velocimetry: Technique and Application to a Spherical Cap Wake Flow, *Applied Scientific Research,* 56(2-3), 157-180.

Chen, R. C. and Fan, L. –S. (1992). Particle image velocimetry for characterizing the flow structure in three-dimensional gas-liquid-solid fluidized beds. *Chem. Eng. Sci*., 47, (13/14), 3615-3622.

Chen, R. C., Reese, J., and Fan, L. –S. (1994). Flow structure in a three-dimensional bubble column and three-phase fluidized bed. *AIChE Journal*, July, 40(7), 1093-1103.

Clark, K.N., (1990). The effect of high pressure and temperature on phase distribution in a bubble column. *Chem. Eng. Sci*., 45, 2301.

Crowe, C., Sommerfeld, M., Tsuji, Y., (c1998). Multiphase Flows with Droplets and Particles, Boca Raton, Fla. CRC Press.

Deckwer, W.-D., Louisi, Y., Zaidi, A. and Ralek, M., (1980). Hydrodynamic properties of the Fischer-Tropsch slurry process, *Ind. Eng. Chem. Process Des. Dev*., 19, 699.

Deckwer, W.D., (1992). Bubble Column Reactors, John Wiley.

Deen, N.G., Hjertager, B.H., and Solberg, T. (2000). Comparison of PIV and LDA measurement methods applied to the gas-liquid flow in a bubble column, 10th Intl. Symp. on applications of laser techniques to fluid mechanics, Lisbon, Portugal.

Dhaouadi, H., Poncin, S., Oinas, P., Hornut, J.M., Wild, G., (1996). Hydrodynamics of an airlift reactor: experiments and modeling. *Chem. Eng. Sci*., 51, 2625-2630.

Fan, L.-S., Yang, G.Q., Lee, D.J., Tsuchiya, K., Luo, X., (1999). Some aspects of high-pressure phenomena of bubbles in liquids and liquid-solid suspensions *Chem. Eng. Sci.*, 54, 4681-4709.

Fialova, M., Ruzicka, M.C. & Drahos, J. (2004). Factors influencing character of bubble bed in bubble column reactors. *Can J. Chem. Eng*., *In Press.*

García-Calvo, E., Letón P., (1991a). A fluid dynamic model for bubble columns and airlift reactors, *Chem. Eng. Sci*., 46, 2947-2951.

García-Calvo, E., Letón P., Arranz M. A., (1991b). Prediction of gas hold up and liquid velocity in airlift loop reactors containing highly viscous Newtonian liquids, *Chem. Eng. Sci*., 46, 2951-2954.

García-Calvo, E., Letón P., (1994). Prediction of fluid dynamics and liquid mixing in bubble columns, *Chem. Eng. Sci*., 49, 3643-3649.

García-Ochoa, J., Khalfet, R., Poncin, S., Wild, G., (1997). Hydrodynamics and Mass Transfer in a suspended solid bubble column with polydispersed high density particles. *Chem. Eng. Sci*., 52, 3827-3834.

Gentile, F., Oleschko, H., Veverka, P., Machon, V., Paglianti, A., Bujalski, W., Etchells, 111 A.W., and Nienow, A.W., (2003). Some effects of particle wettability in agitated solid-gas-liquid systems: Gas-Liquid Mass Transfer and the dispersion of floating solids. *J. Chem. Eng. Japan*, 78, June, 581-587.

Hyndman, C.L., Larachi, F., & Guy, C. (1997). Understanding gas-phase hydrodynamics in bubble columns: a convective model based on kinetic theory. *Chem. Eng. Sci.*, 52, 63–77.

Idogawa, K., Ikeda, K., Fukuda, F. Morooka, S., (1986). Behavior of bubbles of the air-water system in a bubble column under high pressure. *Int. Chem. Eng.*, 26, 468-474.

Idogawa, K., Ikeda, K., Fukuda, F. Morooka, S., (1987). Effect of gas and liquid properties on the behavior of bubbles in a bubble column under high pressure. *Int. Chem. Eng.*, 27, 93-99.

Jamialahmadi, M., & Muller-Steinhagen, H. (1993). Gas hold-up in bubble column reactors. In N. P. Cheremisinoff, (Ed.), *Encyclopedia of fluid mechanics*. Supplement 2., 387–407, Houston: Gulf Publishing Company.

Koide, K., Yasuda, T., Iwamoto, S., & Fukuda, E. (1983). Critical Gas Velocity Required For Complete Suspension of Solid Particles in Solid-Suspended Bubble Columns. *J. Chem. Eng. Japan*, 16(1), 7-12.

Koide, K., Iwamoto, S., Takasaka, Y., Matsuura, S., Takahashi, E., and Kimura, M., (1984). Liquid circulation, gas holdup and pressure drop in bubble column with draught tube. *J. Chem. Eng. Japan*, 17(6), 611-618.

Kojima, H., Sawai, J., Suzuki, H., (1997). Effect of pressure on volumetric mass transfer coefficient and gas holdup in bubble column, *Chem. Eng. Sci.*, 52, 4111-4116.

Krishna, R. P., Wilkinson, P. M., van Dierendonck, L. L., (1991). A model for gas holdup in bubble columns incorporating the influence of gas density on flow regime transitions. *Chem. Eng. Sci.*, 46, 2491-2496.

Krishna, R., de Swart, J.W.A., Ellenberger, J., Martina, G.B., & Maretto, C., (1997). Gas holdup in slurry bubble columns: Effect of column diameter and slurry concentrations. *AIChE J.*, 43(2), 311-447.

Krishna, R., Ellenberger, J., & Maretto, C., (1999). Flow regime transition in bubble columns. *Int. Comm. Heat Mass Transfer*, 26(4), 467-475.

Krishna, R., Urseanu, M.I., de Swart, J.W.A & Ellenberger, J., (2000). Gas holdup in bubble columns: Operation with concentrated slurries versus high viscosity liquid. *Can J. Chem. Eng*., 78, June, 442-447.

Letzel, H. M., Schouten, J. C., Krishna, R., van den Bleek, C. M., (1999 a). Gas holdup and mass transfer in bubble column reactors operated at elevated pressure, *Chem. Eng. Sci.*, 54, 2237-2246.

Letzel, M., & Stankiewicz, A. (1999 b). Gas hold-up and mass transfer in gas-lift reactors operated at elevated pressures, *Chem. Eng. Sci.*, 54, 5153-5157.

Lin, T. -J., Reese, J., Hong, T., and Fan, L. -S. (1996). Quantitative analysis and computation of two-dimensional bubble columns. *AIChE J.*, February, 42(2), 301-318.

Lin, T.-J., Tsuchiya, K., & Fan, L.-S., (1999). On the measurements of regime transition in high pressure bubble columns. *Can J. Chem. Eng*., 77, April, 370-374.

Lin, T.-J., Juang, R.-C., & Chen, C.-C., (2001). Characterizations of flow regime transitions in a high-pressure bubble column by chaotic time series analysis of pressure fluctuation signals. *Chem. Eng. Sci.*, 56, 6241–6247.

Lin, T. J., Chiu, H. T. and Chen, P. C. (2004). Quantitative analysis and computation of the averaged hydrodynamics of an airlift reactor. In press.

Lindken, R.; Gui, L.; Merzkirch, W. (1999). Velocity Measurement in Multiphase Flow by Means of Particle Image Velocimetry, *Chem. Eng. Tech.* 22(3), 202-206.

Luo, X., Jiang, P., & Fan, L.-S. (1997). High pressure three-phase fluidization: Hydrodynamics and heat transfer. *AIChE J*., *43*, 2432.

Luo, X., Lee, D. J., Lau, R., Yang, G., Fan, L. S., (1999). Maximum Stable Bubble Size and Gas Holdup in High-Pressure Slurry Bubble Columns, *AIChE J*., 45, 665-680.

Mudde, R. F., Lee, D. J., Reese, J., and Fan, L. –S. (1997 a). Role of coherent structures on Reynolds stresses in a 2-D bubble column. *AIChE Journal*, April, 43(4), 913-926.

Mudde, R. F., Groen, J. S. and Van Den Akker, H. E. A., (1997 b). Liquid velocity field in a bubble column: LDA experiments. *Chem. Eng. Sci.*, 52(21-22), 4217-4224.

Onno Kramer, (2002). Applied process science. http://www. Utwente.nl.

Olmos, E., Gentric, C. and Midoux, N. (2003) Identification of flow regimes in a flat gas-liquid bubble column via wavelet transform. *Can J. Chem. Eng.*, 81, June-August, 382-387.

Reese, J., and Fan L.-S., (1994) Transient flow structure in the entrance region of a bubble column using particle image velocimetry. *Chem. Eng. Sci.*, 49(24B), 5623-5636.

Reilly, I.G., Scott, D.S., De Bruijn, T.J.W., and Macintyre, D. (1994) The role of gas phase momentum in determining gas holdup and hydrodynamic flow regimes in bubble column operations. *Can J. Chem. Eng.*, 72, 3-12.

Ruzicka, M., Zahradnik, J., Drahos, J., Thomas, N.H., (2001 a). Homogeneous_ heterogeneous regime transition in bubble columns. *Chem. Eng. Sci.,* 56, 4609-4626.

Ruzicka, M.C., Drahos, J., Fialova, M., Thomas, N.H., (2001 b) Effect of bubble column dimensions on flow regime transition. *Chem. Eng. Sci.* 56, 6117-6124.

Sarrafi, A., Jamialahmadi, M., Steinhagen, H.M., & Smith, J.M., (1999). Gas holdup in homogeneous and heterogeneous gas-liquid bubble column reactors. *Can J. Chem. Eng.*, 77 (February), 11-21.

Saxena, S. C. & Chen, Z. D., (1994). Hydrodynamics and heat transfer of baffled and unbaffled slurry bubble columns. *Rev. in Chem. Eng.*, 10(3-4), 195.

Shah, Y. T., Deckwer, W. D., (1983). Hydrodynamics of bubble columns. *Handbook of Fluids in Motion* (eds N. P. Cheremisinoff and R. Gupta), Chap. 22, 583-620. Ann Arbor Science, Ann Arbor.

Shnip, A.I., Kolhatkar, R.V., Swamy, D. & Joshi, J.B., (1992). Criteria for The transition from the homogeneous to the heterogeneous regime in two-dimensional bubble column reactors. *Int. J. Multiphase Flow*, 18(5), 705-726.

Tsuchiya, K. and Nakanishi, O., (1992). Gas holdup behavior in a tall bubble column with perforated plate distributors. *Chem. Eng. Sci.*, 47, 3347–3354.

Tzeng, J. –W., Chen, R. C., and Fan, L. –S. (1993). Visualization of flow characteristics in a 2-D bubble column and three-phase fluidized bed. *AIChE Journal*, May, 39(5), 733-743.

Van Benthum, W.A.J., Van der Lans, R.G.J.M., Van Loosdrecht, M.C.M., Heijnen, J.J., (1999). Bubble recirculation regimes in an internal-loop airlift reactors. *Chem. Eng. Sci.*, 54, 3995-4006.

Vial, C., Poncin, S., Wild, G., Midoux, N., (2001 a). A Simple method for regime identification and flow characterization in bubble columns and airlift reactors. *Chem. Eng. & Proc.*, 40, 135-151.

Vial, C., Laine, R., Poncin, S., Midoux, N. and Wild, G. (2001 b). Influence of gas distribution and regime transitions on liquid velocity and turbulence in a 3-D bubble column. *Chem. Eng. Sci.*, 56, 1085-1093.

Wallis, G.B., (1969). One-dimensional two-phase flow, McGraw-Hill, New York.

Wild, G., Poncin, S., Li, H.-Z., Olmos, E., (2003). Some aspects of the hydrodynamics of bubble columns. *International Journal of Chemical Reactor Engineering*, 1, R7, 1-36.

Wilkinson, P. M., Spek, A. P, Van Dierendonck, L. L., (1992). Design parameters estimation for scale-up of high-pressure bubble columns. *AIChE J.,* 38(4), 544-553.

Yamashita, F., (1998). Effect of clear liquid height and gas inlet height on gas holdup in a Bubble column. *J. Chem. Eng. Japan*, 31, 285-288.

Zahradnik, J., Fialova, M., Ruzicka, M., Drahos, J., Kastanek, F., & Thomas, N.H., (1997). Duality of the gas- liquid flow regimes in bubble column reactors. *Chem. Eng. Sci.*, 52(21/22), 3811-3826.

APPENDIX
FOR TIME AVERAGED SURFACE PLOT PROGRAM

```
clear;
format long;

N=4600;
averu=zeros(N,1);
averv=zeros(N,1);

m=zeros(N,1);

for num=0:1:29
   fnum=num2str(num);
   if(num<10)
      fparta='C:\Document\Small column\PIV results\DT and WDT
results\DTbotthree\DTbotthree0000';
   else
      fparta='C:\Document\Small column\PIV results\DT and WDT
results\DTbotthree\DTbotthree000';
   end
   filename=strcat(fparta,fnum,'.vec');
   fp=fopen(filename,'r');
   total=fscanf(fp,'%s');
   fsize=ftell(fp);
   frewind(fp);
   title=fscanf(fp,'%s',21);
   i=0;
   while (ftell(fp)<=(fsize-21-4))
      i=i+1;
      x(i)=fscanf(fp,'%f',1);
      c=fscanf(fp,'%s',1);
      y(i)=fscanf(fp,'%f',1);
      c=fscanf(fp,'%s',1);
      u(i)=fscanf(fp,'%f',1);
      c=fscanf(fp,'%s',1);
      v(i)=fscanf(fp,'%f',1);
      c=fscanf(fp,'%s',1);
      state(i)=fscanf(fp,'%d',1);
   end
   fclose(fp);

   for k=1:1:i
      if(state(k)>0)
         m(k)=m(k)+1;
         averu(k)=(averu(k)*(m(k)-1)+u(k))/m(k);
         averv(k)=(averv(k)*(m(k)-1)+v(k))/m(k);
      else
```

```
        continue;
      end
   end

 num
end

fp1=fopen('C:\Document\Small column\PIV results\DT and WDT
results\DTbotthree\average.txt','w');
for k=1:1:i
   fprintf(fp,'%d %f %f %f %f\n', k, x(k), y(k), averu(k), averv(k));
end
fclose(fp1);

for k=1:1:i
   avufinal(k)=averu(k);
   avvfinal(k)=averv(k);
end

xx=sort(x);
inter=-y;
inter2=sort(inter);
yy=-inter2;
mm=1;
nn=1;
xxx(mm)=xx(1);
yyy(nn)=yy(1);
for kk=2:1:i
   if(xx(kk)~=xx(kk-1))
      mm=mm+1;
      xxx(mm)=xx(kk);
   end

   if(yy(kk)~=yy(kk-1))
      nn=nn+1;
      yyy(nn)=yy(kk);
   end
end

avukkk=zeros(nn,mm);
avvkkk=avukkk;

for kkk=1:1:nn
   for kkkk=1:1:mm
      avukkk(kkk,kkkk)=avufinal(mm*(kkk-1)+kkkk);
      avvkkk(kkk,kkkk)=avvfinal(mm*(kkk-1)+kkkk);
   end
end

[xxxx,yyyy]=meshgrid(xxx,yyy);
```

```
quiver(xxxx,yyyy,2*avukkk,2*avvkkk,2.5,'b');

figure;
surf(xxxx,yyyy,avvkkk);
```